Environment International 137 (2020) 105581

Contents lists available at ScienceDirect

Environment International

journal homepage: www.elsevier.com/locate/envint

# Probabilistic human health risk assessment of perfluorooctane sulfonate (PFOS) by integrating *in vitro*, *in vivo* toxicity, and human epidemiological studies using a Bayesian-based dose-response assessment coupled with physiologically based pharmacokinetic (PBPK) modeling approach

Wei-Chun Chou, Zhoumeng Lin*

*Institute of Computational Comparative Medicine (ICCM), Department of Anatomy and Physiology, College of Veterinary Medicine, Kansas State University, Manhattan, KS 66506, United States*

ARTICLE INFO

Handling Editor: Adrian Covaci

*Keywords:*
Dose-response analysis
Interspecies extrapolation
Perfluoroalkyl substances (PFAS)
Perfluorooctane sulfonate (PFOS)
Physiologically based pharmacokinetic (PBPK) modeling
Risk assessment

ABSTRACT

*Background:* Environmental exposure to perfluorooctane sulfonate (PFOS) is associated with various adverse outcomes in humans. However, risk assessment for PFOS with the traditional risk estimation method is faced with multiple challenges because there are high variabilities and uncertainties in its toxicokinetics and toxicity between species and among different types of studies.

*Objectives:* This study aimed to develop a robust probabilistic risk assessment framework accounting for inter-species and inter-experiment variabilities and uncertainties to derive the human equivalent dose (HED) and reference dose for PFOS.

*Methods:* A Bayesian dose-response model was developed to analyze selected 34 critical studies, including human epidemiological, animal *in vivo*, and ToxCast *in vitro* toxicity datasets. The dose-response results were incorporated into a multi-species physiologically based pharmacokinetic (PBPK) model to reduce the toxicokinetic/toxicodynamic variabilities. In addition, a population-based probabilistic risk assessment of PFOS was performed for Asian, Australian, European, and North American populations, respectively, based on reported environmental exposure levels.

*Results:* The 5th percentile of HEDs derived from selected studies was estimated to be 21.5 (95% CI: 10.6–36.3) ng/kg/day. After exposure to environmental levels of PFOS, around 50% of the population in all studied populations would likely have > 20% of increase in serum cholesterol, but the effects on other endpoints were estimated to be minimal (< 10% changes). There was a small population (~10% of the population) that was highly sensitive to endocrine disruption and cellular response by environmental PFOS exposure.

*Conclusion:* Our results provide insights into a complete risk characterization of PFOS and may help regulatory agencies in the reevaluation of PFOS risk. Our new probabilistic approach can conduct dose-response analysis of different types of toxicity studies simultaneously and this method could be used to improve risk assessment for other perfluoroalkyl substances (PFAS).

*Abbreviations:* ALC, average liver concentration; ASC, average serum concentration; AUC, area under the curve; BBMD, Bayesian approach in benchmark dose (BMD) analysis; BMD, benchmark dose; CR, cellular response; Css, steady-state concentration; EFSA, European Food Safety Authority; EP, exceedance probability; ER, endocrine disruption; HBEpC, primary human bronchial epithelial cells; HCASMC, human coronary artery smooth muscle cells; HED, human equivalent dose; HepG2, human hepatocellular carcinoma cells; ImmunoTox, immunotoxicity; IVIVE, *in vitro* to *in vivo* extrapolation; LOAEL, lowest observed adverse effect level; MCMC, Markov chain Monte Carlo; MOA, mode of action; NeuroTox, neurotoxicity; NHANES, National Health and Nutrition Examination Survey; NOAEL, no-observed-adverse-effect-level; NRC, National Research Council; PBPK, physiologically based pharmacokinetic; PFAS, perfluoroalkyl substances; PFOS, perfluorooctane sulfonate; POD, point of departure; RfD, reference dose; SC, serum cholesterol; TD, threshold dose; TDI, tolerable daily intake; U.S. EPA, United States Environmental Protection Agency; UBA, German Federal Environment Agency; WHO, World Health Organization

* Corresponding author at: 1800 Denison Avenue, P200 Mosier Hall, Institute of Computational Comparative Medicine (ICCM), Department of Anatomy and Physiology, College of Veterinary Medicine, Kansas State University, Manhattan, KS 66506, United States.

*E-mail addresses:* weichunc@vet.k-state.edu (W.-C. Chou), zhoumeng@ksu.edu (Z. Lin).

https://doi.org/10.1016/j.envint.2020.105581
Received 12 October 2019; Received in revised form 21 January 2020; Accepted 12 February 2020
Available online 19 February 2020

## 1. Introduction

Perfluorooctane sulfonate (PFOS) has been produced since the 1950s and are widely used in commercial and industrial products, including cookware, furniture, household cleaners, clothing and fire-fighting foam (Paul et al., 2009; Sunderland et al., 2019). Despite the production and the use of PFOS has been phased out in the U.S. since 2002 (U.S. EPA, 2009a; FDA, 2011; Renner, 2008), a growing number of studies have shown it is still frequently detected in the environment (Hu et al., 2016; Sunderland et al., 2019) and human samples (Calafat et al., 2007; Mamsen et al., 2019; Pérez et al., 2013). Because of PFOS' widespread presence and worldwide exposure of humans, there is an increasing concern on its potential adverse health effects.

A growing number of studies in rodents and non-human primates have reported that excessive PFOS exposure causes hepatic effects, endocrine effects, immunological dysfunction, and developmental effects (Zeng et al., 2019). For example, numerous studies have shown that short-term (0.14–6.34 mg/kg/day for 4 weeks) (Curran et al., 2008), subchronic (0.04–1.33 mg/kg/day for 14 weeks) (Seacat et al., 2003) and long-term PFOS exposure (0.5–20 mg/kg/day for 105 weeks) (Butenhoff et al., 2012) cause hepatic toxicities, including increase of liver weight, histopathological changes, or decrease of serum cholesterol. Regarding effects on the endocrine and immune systems, PFOS exposure decreases the total thyroxine (T4) at the doses of ≥1.33 mg/kg/day and ≥1.43 mg/kg/day in male and female rats, respectively (Curran et al., 2008), which is consistent with the other studies in rats and mice (Lau et al., 2003; Seacat et al., 2003). For developmental effects, several subchronic studies (63–84 days) in rats (dose range of 0.1–10 mg/kg/day) and mice (dose range of 1–20 mg/kg/day) have shown that gestational exposure to PFOS results in decreased pre- and post-natal survival of offspring, and other effects (e.g., reduced fetal weight, delayed bone ossification, and reduced neonatal survival) (Butenhoff et al., 2009; Lau et al., 2003; Luebker et al., 2005a, 2005b). In humans, the majority of published epidemiological studies (EFSA, 2018; Eriksen et al., 2013; Frisbee et al., 2010; Geiger et al., 2014; Nelson et al., 2010; Steenland et al., 2009) have reported a positive association between PFOS and increases in total cholesterol in the general populations at mean serum levels of 0.0224–0.0361 μg/mL. For *in vitro* studies, the potential toxicities of PFOS have also been examined via high-throughput screening in the U.S. Environmental Protection Agency (EPA) ToxCast program with a broad dose range (1 nM to 100 μM), and PFOS exposure has been associated with several toxicity endpoints, including PPAR/PXR/RAR receptors, neurotoxicity, aquatic toxicity, immunotoxicity, endocrine disruption, and activation of cytochrome P450s (U.S. EPA, 2016).

The health-protective exposure values (e.g., reference dose [RfD] or tolerable daily intake [TDI]) have been developed to be protective for chronic exposure to PFOS based on animal or human studies. For example, U.S. EPA developed a RfD of 77 ng/kg/day in 2009 based on decreased serum T3 levels observed in a 28-week monkey study (U.S. EPA, 2009b). Accounting for the differences of toxicokinetics for PFOS between animals and humans, U.S. EPA released a new RfD of 20 ng/kg/day in 2016 based on a rat developmental study (U.S. EPA, 2016). Most recently, based on human epidemiological studies, European Food Safety Authority (EFSA) released a TDI of 1.8 ng/kg/day in 2018 (EFSA, 2018). Both estimations of points of departure (PODs), based on whether animal or human studies, have their respective strengths and limitations. For example, the differences of toxicokinetic properties for PFOS between animals and humans make it difficult to extrapolate dosimetry from animal studies to humans. Epidemiological studies are limited in their ability to establish causality for the derivation of RfD. Given these differences in the estimation of health-protective exposure values between epidemiological and experimental studies, a key issue is how to create an integrated approach that can unify different toxicity endpoints from different types of critical studies to support the determination of health-protective exposure values. In addition, the dosimetry extrapolation across species accounting for inter/intra-species toxicokinetic differences needs to be considered.

In order to address the abovementioned knowledge gaps, this study developed a Bayesian dose-response model to analyze a comprehensive set of toxicity data, including human epidemiological studies, animal *in vivo* studies, and *in vitro* assays from U.S. EPA ToxCast program to determine probabilistic PODs for PFOS for each endpoint. A recently developed multi-species PBPK model for PFOS (Chou and Lin, 2019) was then used to convert the PODs into human equivalent doses (HEDs) based on U.S. EPA's guidance (U.S. EPA, 2016). Finally, this probabilistic risk assessment approach was applied to conduct a population-based risk estimation based on the endpoints from human and ToxCast studies and based on the reported serum PFOS concentrations in the general populations from different countries. All model codes and raw data are provided in the Supplemental Materials to allow to reproduce our results and facilitate the application and extrapolation of this framework to other perfluoroalkyl substances (PFAS).

## 2. Methods

### 2.1. Study framework

Fig. 1 represents a conceptual framework depicting the general process of this study, including hazard identification, dose-response analysis, exposure assessment, and risk characterization. Of note, this study integrated Bayesian dose-response analysis (Chiu et al., 2017; Shao and Shapiro, 2018) with our recently developed multi-species PBPK model (Chou and Lin, 2019) to derive HEDs based on human epidemiological, animal *in vivo* toxicity, and ToxCast *in vitro* data.

### 2.2. Hazard identification

Studies were included in our analyses based on the following considerations. First, to consider the toxicodynamic variability between study populations, between *in vitro* and *in vivo*, and between animals and humans, we included diverse toxicity studies ranging from *in vitro*, animal *in vivo* toxicity, to human epidemiological studies. Second, each selected study should include at least 3 dose groups (or concentration groups) with at least one group that produced an effect that was more than 10% difference from the control group. This is needed in order to generate a meaningful nonlinear dose-response curve. Third, the developmental toxicity studies were excluded in our analyses because our PBPK model is only used for adult animals and humans (Chou and Lin, 2019). Fourth, the selection of endpoints was dependent on the weight of evidence provided by peer-reviewed literature. To be more specific, recent EFSA report has concluded that it is likely there is a causal association between PFOS exposure and increased serum total cholesterol based on a comprehensive review for human epidemiological studies (EFSA, 2018). Accordingly, this study collected the same three critical human studies used by EFSA (Eriksen et al., 2013; Nelson et al., 2010; Steenland et al., 2009) and one additional study (Château-Degat et al., 2010) that met the selection criteria of EFSA (i.e., over 500 subjects in the cohort study), so that our results would be comparable to the guidance values from EFSA. While selection bias may occur, EFSA expert panel has concluded that it is unlikely the use of these studies will affect the association between PFOS and increased serum total cholesterol (EFSA, 2018).

In animals, increased liver weight has been concluded as the hallmark response following PFOS exposure (EFSA, 2018; U.S. EPA, 2016). Therefore, animal studies reporting increased liver weight were considered in the dose-response analysis. The selected animal and human studies are listed in Table 1. Ideally, chronic animal toxicity studies (if available) should be used to derive POD and RfD, but the selected animal studies were subchronic toxicity studies with exposure duration ranging from 28 to 182 days. These subchronic studies were selected due to lack of chronic studies that were suitable for dose-response

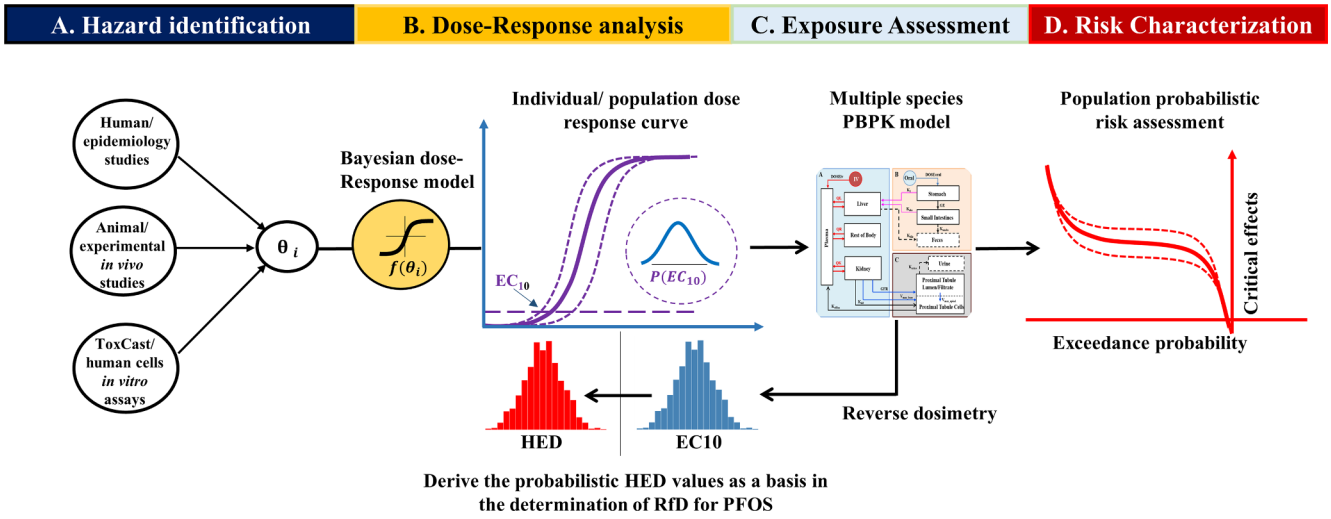


**Fig. 1.** Schematic illustration of the study framework. (A) The first step of hazard identification is to evaluate the potential toxicity and collect the dose-response datasets from human, animal and ToxCast *in vitro* studies. (B) The second step is to construct the Bayesian dose-response model to derive EC10 (i.e., effective concentration or dose resulting in 10% of changes) as PODs (i.e., point of departures). (C) A multi-species PBPK model was used to convert the PODs into the HED (i.e., human equivalent dose) with a reverse dosimetry approach. (D) Finally, the risk can be characterized using the exceedance probability approach.

analysis for the endpoint of increased liver weight. In the literature, we only found one chronic study in which rats were fed with 0, 0.5, 2, 5, and 20 ppm diet for up to 104 weeks and animals were sacrificed on Weeks 4, 14, and 53 (interim sacrifices), with terminal sacrifice between Weeks 103 and 106 (Butenhoff et al., 2012; Seacat et al., 2003). Liver weight data were not available on Weeks 103–106. The liver weight was significantly increased on Week 53, but the data were only available at the control and 20 ppm groups, thus these data were not suitable for dose-response analysis (Butenhoff et al., 2012; U.S. EPA, 2016). Also, these subchronic studies were selected because they were used as critical studies for the derivation of RfD by U.S. EPA (U.S. EPA, 2016) and other agencies (UK COT, 2006; EFSA, 2008). We chose the same critical studies so that our results would be comparable to EFSA's and U.S. EPA's guidance values. In addition, an uncertainty factor for extrapolation from the subchronic to the chronic exposure duration of 1-fold, rather than the default uncertainty factor of 10-fold for many other chemicals, was used in the present study because the PODs were based on the average serum concentrations and this uncertainty factor was used and well justified in the latest U.S. EPA guidance document (U.S. EPA, 2016).

In line with the toxicology testing paradigm in the 21st century proposed by the National Research Council (NRC) and implemented by multiple U.S. federal agencies (i.e., the Tox21 program) (Kavlock et al., 2019; NRC, 2007), the present study incorporated biochemical- and human cell-based high throughput *in vitro* assays from U.S. EPA's ToxCast program into the dose-response analysis. Note that not all biological pathway perturbations would lead to adverse human health effects (Krewski et al., 2019). Biological pathways that are expected to lead to adverse health effects *in vivo* when they are sufficiently altered are termed toxicity pathways. Based on the recent U.S. EPA report (U.S. EPA, 2016), the present study selected ToxCast *in vitro* assays that are related to PFOS toxicity and have been used in the U.S EPA risk assessment so that our results are comparative to the results from U.S. EPA. These representative assays evaluate different molecular events to be associated with several adverse effects based on the categories defined by U.S. EPA guidance (U.S. EPA, 2016), including "PPAR/PXR/RAR Receptors", "Neurotoxicity", "Immunotoxicity", and "Endocrine Disruption". In addition, the PFOS-activated assays also involved the effects of oxidative stress, mitochondrial toxicity, cell loss, and mitotic arrest. These assays were categorized as "cellular response" in our study. A list of all selected studies is presented in Tables 1 and 2. Additional description of selected studies is provided in the Supplementary Materials.

### 2.3. Dose-response analysis

#### 2.3.1. Data preprocessing

Since the dose-response data were of different types with different endpoints and from different experiments/sources, we normalized the unit of response across all studies for the purpose of generalization. Based on the definition of benchmark dose (Haber et al., 2018), the risk (additional risk) can be expressed as the incremental changes over background. All the data included in this study have internal references, such as the control group in the human epidemiological studies and animal *in vivo* studies, and fold change in ToxCast *in vitro* data. To account for this in the model, we normalized the measured response as:

$$y_{i,j} = \left(\frac{r_{i,j} - r_{0,j}}{r_{0,j}}\right) \times 100 \quad (1)$$

where $y_{i,j}$ represents as the incremental changes (percentage of incremental increase of the response over the control group at dose $d_0$) at dose group $i$ in experiment $j$; $r_{i,j}$ is the response at exposure group $i$ in experiment $j$; and $r_{0,j}$ is the response at the control group in experiment $j$. This approach normalizes the background risk to be 0. In the human studies, the 170 mg/dL was used as $r_{0,j}$ based on the definition of normal lipid value recommendation from American Heart Association (Grundy et al., 2019).

Two different dose-response models were used in this work, a modified version of the Hill model recommended by the U.S. EPA BMD guidance (U.S. EPA, 2012) was adopted to describe the continuous dose-response data in humans,

$$f(d;\theta) = \frac{b \cdot d^c}{a^c + d^c} \quad (2)$$

and a logarithmic form of the Hill model was used to fit the dose-response data of animal *in vivo* and ToxCast *in vitro* studies:

$$f(d;\theta) = \frac{b}{1 + \exp\{-c[\log(d) - \log(a)]\}} \quad (3)$$

where $f(d;\theta)$ represents the expected response at dose $d$, and $\theta = (a, b, c)$. In both models, the parameter $a$ represents the concentration or the dose achieving the half-maximal response (i.e., EC50), $b$ is the maximum response (i.e., Emax), $c$ is the Hill coefficient (reflects the shape of the curve). To evaluate the model performance, we calculated

**Table 1**
Key information of selected animal *in vivo* and human studies in the dose-response analysis for PFOS.

| Assigned no. | Reference | Exposure route | Species or Human population | Category/Critical endpoint |
|---|---|---|---|---|
| Animal_1 | Seacat et al. (2002) | Oral (capsule) | Cynomolgus monkeys | Hepatic toxicity/Increased liver weight |
| Animal_2 | Seacat et al. (2003) | Oral (in diet) | Sprague Dawley rats | Hepatic toxicity/Increased liver weight |
| Animal_3 | Curran et al. (2008) | Oral (in diet) | Sprague Dawley rats | Hepatic toxicity/Increased liver weight |
| Animal_4 | Dong et al. (2009) | Oral gavage | C57BL/6 mice | Hepatic toxicity/Increased liver weight |
| Animal_5 | Dong et al. (2011) | Oral gavage | C57BL/6 mice | Hepatic toxicity/Increased liver weight |
| Animal_6 | Lefebvre et al. (2008) | Oral (in diet) | Sprague Dawley rats | Hepatic toxicity/Increased liver weight |
| Human_1 | Steenland et al. (2009) | Unknown | Human/High-exposure community (C8-health project with the adults ≥18 years old, n = 46,294) | Lipotoxicity/Increased serum cholesterol |
| Human_2 | Eriksen et al. (2013) | Unknown | Human/General population (Danish cohort, n = 753) | Lipotoxicity/Increased serum cholesterol |
| Human_3 | Nelson et al. (2010) | Unknown | Human/General population (NAHENS 2003–2004, n = 860) | Lipotoxicity/Increased serum cholesterol |
| Human_4 | Château-Degat et al. (2010) | Unknown | Human/General population (Inuit population, n = 723) | Lipotoxicity/Increased serum cholesterol |

the adjusted R-squared (Adj. $R^2$) and relative absolute error (RAE) to provide a quantitative measure in the model evaluation. An estimated Adj $R^2 > 0.5$ and RAE $< 1$ indicate that the dose-response model fits with the measured data adequately.

#### 2.3.2. Bayesian dose-response model

In this study, we proposed a Bayesian dose-response model to quantify inter-study/population variability through placing a hierarchical structure on parameters "*a*" in the Eqs. (2) and (3). In the hierarchical structure (Fig. S1 in Supplementary Materials), our proposed model accounts for variability within each experiment (experiment-specific level), variability between studies (study-specific level), and variability in the population (population level). From Bayes' theorem, the joint posterior distribution of the parameter $p(a_j, \mu_a, \sigma_a, b, c|y_{ij})$ is proportional to the likelihood of observed data multiplied by the prior distribution of the parameters:

$$p(a_j, \mu_a, \sigma_a, b, c|y_{ij}) \propto p(y_{ij}|a_j, \mu_a, \sigma_a, b, c)\cdot p(a_j|\mu_a, \sigma_a)\cdot p(\mu_a)\cdot p(\sigma_a)\cdot p(b)\cdot p(c) \quad (4)$$

where the $p(y_{ij}|a_j, \mu_a, \sigma_a, b, c)$ is the likelihood function, which can be written as a logarithmic format $log[p(y_{ij}|a_j, \mu_a, \sigma_a, b, c)]$ $N(log[f(d_{ij}; a_j, \mu_a, \sigma_a, b, c)], \varepsilon_{ij})$ by normal distribution with variance $\varepsilon$ over the dose levels d. To be more specifically, the dose-response model f based on a set of prior parameters $(a_j, \mu_a, \sigma_a, a, c)$ was used to predict the measured response $y_{ij}$ in the study j at the dose level i, with the random effects $\varepsilon_{ij}$ $N(0, \sigma^2)$. The prior distribution of informative parameter "a" was assigned as lognormal prior, which can be denoted as joint prior probability $p(a_j|\mu_a, \sigma_a) = LN(\mu_a, \sigma_a)$. The use of lognormal distribution ensured positive values of the parameters and realistic skewness. Each of the hyper-parameters such as the population mean $\mu_a$ and standard deviation $\sigma_a$ of informative parameter a was assigned an independent prior distribution with half-normal and half-Cauchy distribution, which specify as: $p(\mu_a) = N(0, S_{\mu_a})$ and $p(\sigma_a) = Cauchy(0, S_{\sigma_a})$. We set $S_{\mu_a}$ as the arbitrary values to reflect vague (flat) priors, and assigned $S_{\sigma_c}$ as the weakly informative priors based on previous studies (Gelman, 2006). Parameters "b" and "c" in Eq. (3) were distinguished as non-informative priors with uniform distribution with data-driven upper bounds and lower bounds such as $p(b) = Unif(b_{lower}, b_{upper})$ and $p(c) = Unif(c_{lower}, c_{upper})$. The settings of priors and details on the uniform distributions used in the dose-response model were described in detail in the Supplemental Materials (Section 2.1 Settings of priors for model parameters).

The proposed model was programed with R (version 3.5.3) using R package RStan (Carpenter et al., 2017). The MCMC sampling process consisted of four different Markov chains sampled for 10,000 iterations each. The first 5000 iterations for each chain was disregarded as burn-in, resulting in a posterior sample size of 5000. The convergence of the MCMC sampling was judged by the potential scale reduction statistic $\widehat{R}$ provided from the output of Rstan.

### 2.4. Exposure assessment: multi-species PBPK modeling-based reverse dosimetry analysis

In the exposure assessment, the PBPK model was used for the estimation of human equivalent doses (HEDs) based on the EC10 values derived from human, animal and ToxCast *in vitro* studies using a reverse dosimetry approach (Cheng et al., 2018; Lin et al., 2016; Lyons et al., 2008; Tan et al., 2007; Wambaugh et al., 2018; Wetmore et al., 2012). The recently validated multi-species PBPK model (Chou and Lin, 2019) was implemented here to quantify the internal dosimetry and reduce the uncertainty of interspecies toxicokinetics for PFOS. Note that for ToxCast *in vitro* studies, the *in vitro* EC10 concentrations were based on the nominal concentrations in the culture medium based on previous *in vitro* to *in vivo* extrapolation (IVIVE) studies (Wetmore et al., 2012, 2013, 2015). The use of nominal concentrations in this analysis is mainly because only the nominal concentrations are available from the

**Table 2**
Key information on the selected ToxCast *in vitro* assays in the dose–response analysis for PFOS.

| Assigned no. | ToxCast assay | Normalization | Cell type/Tissue | Gene Symbol | Endpoint category |
|---|---|---|---|---|---|
| ToxCast_1 | ATG_PPRE_CIS_up | log2-fold-induction | Human HepG2[a] cell line | PPARE | PPAR activation |
| ToxCast_2 | ATG_PPARa_TRANS_up | log2-fold-induction | Human HepG2 cell line | PPARA | PPAR activation |
| ToxCast_3 | ATG_PPARg_TRANS_up | log2-fold-induction | Human HepG2 cell line | PPARG | PPAR activation |
| ToxCast_4 | NVS_GPCR_h5HT5A | Percent activity | Cell-free assay | HTR5A | Neurotoxicity |
| ToxCast_5 | NVS_GPCR_h5HT6 | Percent activity | Cell-free assay | HTR6 | Neurotoxicity |
| ToxCast_6 | NVS_GPCR_h5HT7 | Percent activity | Cell-free assay | HTR7 | Neurotoxicity |
| ToxCast_7 | NVS_GPCR_hAdoRA2a | Percent activity | Cell-free assay | ADORA2A | Neurotoxicity |
| ToxCast_8 | NVS_GPCR_hAdra2C | Percent activity | Cell-free assay | ADRA2C | Neurotoxicity |
| ToxCast_9 | NVS_GPCR_hAdrb1 | Percent activity | Cell-free assay | ADRB1 | Neurotoxicity |
| ToxCast_10 | BSK_SAg_CD40_down | log10-fold-induction | HCASMC[b] | CD40 | Immunotoxicity |
| ToxCast_11 | BSK_BE3C_IP10_down | log10-fold-induction | HBEpC[c] | CXCL10 | Immunotoxicity |
| ToxCast_12 | BSK_BE3C_IL1a_down | log10-fold-induction | HBEpC | IL1A | Immunotoxicity |
| ToxCast_13 | BSK_LPS_IL8_up | log10-fold-induction | HCASMC | CXCL8 | Immunotoxicity |
| ToxCast_14 | BSK_3C_uPAR_down | log10-fold-induction | HCASMC | PLAUR | Immunotoxicity |
| ToxCast_15 | BSK_CASM3C_VCAM1_down | log10-fold-induction | HCASMC | VCAM1 | Immunotoxicity |
| ToxCast_16 | OT_ER_ERaERb_0480 | Percent activity | HEK293cell line | ESR α | Endocrine disruptors |
| ToxCast_17 | ATG_ERa_TRANS_up | log2-fold-induction | Human HepG2 cell line | ESR α | Endocrine disruptors |
| ToxCast_18 | ATG_ERE_CIS_up | log2-fold-induction | Human HepG2 cell line | ESR α | Endocrine disruptors |
| ToxCast_19 | NVS_NR_hTRa_Antagonist | Percent activity | Cell-free assay | THRA | Endocrine disruptors |
| ToxCast_20 | APR_HepG2_CellLoss_24h_dn | log2-fold-induction | Human HepG2 cell line | – | Cytotoxicity/Cellular response |
| ToxCast_21 | APR_HepG2_MitoMass_24h_dn | log2-fold-induction | Human HepG2 cell line | – | Mitochondria/Cellular response |
| ToxCast_22 | APR_HepG2_OxidativeStress_24h_up | log2-fold-induction | Human HepG2 cell line | – | Oxidative stress/Cellular response |
| ToxCast_23 | APR_HepG2_p53Act_24h_up | log2-fold-induction | Human HepG2 cell line | TP53 | DNA binding/Cellular response |
| ToxCast_24 | APR_HepG2_MitoticArrest_24h_up | log2-fold-induction | Human HepG2 cell line | – | Cell cycle/Cellular response |

[a] HepG2: Human hepatocellular carcinoma cells.
[b] HCASMC: Human coronary artery smooth muscle cells.
[c] HBEpC: Primary human bronchial epithelial cells.

ToxCast program. Also, there are a variety of *in vitro* assays, including cell-free biochemical and cell-based assays with different types of cells (e.g., transformed and primary cells), which makes it challenging to assess the free concentration of the chemical in each assay. This limitation of using *in vitro* assays, especially the nominal concentration in risk assessment is further discussed in the Discussion section.

Two different dose metrics, average serum concentration ($ASC_{human}$) and steady-state serum concentration ($C_{ss}$) were used in the reverse dosimetry analysis to convert the EC10 from human epidemiological studies and ToxCast *in vitro* studies, respectively, into the HED using Eq. (5) (Rotroff et al., 2010; Wetmore et al., 2012). Note that the consideration of the free concentration (or unbound concentration) of PFOS in the plasma is important in the calculation of $ASC_{human}$ and $C_{ss}$; this has been considered and described in detailed in our PBPK modeling paper (Chou and Lin, 2019).

$$\mathrm{HED}\left(\frac{\frac{\mathrm{mg}}{\mathrm{kg}}}{\mathrm{day}}\right) = \mathrm{Human}\ \ (\mathrm{ng/mL})\ \ \mathrm{or}\ \ \mathrm{ToxCast}\ \ \mathrm{EC10}\ \ (\mu\mathrm{M}) \cdot \frac{1\left(\frac{\mathrm{mg}}{\mathrm{kg}}\right)\Big/\mathrm{day}}{\mathrm{ASC_{human}(ng/mL)}\ \ or\ \ C_{ss}(\mu\mathrm{M})} \tag{5}$$

In the Eq. (5), HED is linearly related to the human (ng/mL) and *in vitro* EC10 ($\mu$M) and inversely related to the $ASC_{human}$ or $C_{ss}$ after exposure to a daily dose of 1 mg/kg/day. To calculate $ASC_{human}$, we firstly simulated the plasma AUC at a dose of 1 mg/kg/day for 50 years, and then calculated using the equation (i.e., $ASC_{human}$ [ng/mL] = AUC [μg/mL * h] * 1000/(Exposure duration [days] * 24 h/1 day)) based on U.S. EPA report (U.S. EPA, 2016). Similarly, $C_{ss}$ was obtained via a PBPK simulation at the dose of 1 mg/kg/day for 50 years. Based on the assumption of IVIVE, the HED derived from *in vitro* studies was used to assess whether *in vitro* bioactivity would be expected at the dose-equivalent level of human exposure.

For animal studies, since the target organ is liver, the HED value was estimated based on the dosimetry in liver according to the following formula:

$$\mathrm{HED}\left(\frac{\frac{\mathrm{mg}}{\mathrm{kg}}}{\mathrm{day}}\right) = \mathrm{Animal}\ \ \mathrm{EC10}\left(\frac{\mathrm{mg}}{\mathrm{kg}}\Big/\mathrm{day}\right) \cdot \frac{\mathrm{ALC_{animal}(ng/mL)}}{\mathrm{ALC_{human}(ng/mL)}} \tag{6}$$

To calculate the HED, the AUC values in liver corresponding to a daily dose of 1 mg/kg/day for one year was firstly predicted in animals using the multi-species PBPK model, and then the average liver concentration in animals ($ALC_{animal}$) and humans ($ALC_{human}$) was calculated from the ASC equation (described above). Then HED was calculated using animal EC10 distributions multiplied the ratio of ALC values between animals and humans (Andersen et al., 2002; Chou and Lin, 2019). The purpose of calculating $ALC_{animal}/ALC_{human}$ was to account for the interspecies toxicokinetic uncertainty/variability in the PFOS dosimetry. Also, the endpoint of increased liver weight in animals is likely a function of cumulative dose, and ALC is a relatively stable representative dose metric because ALC is derived from AUC (i.e., cumulative dose) divided by the exposure duration (U.S. EPA, 2016). The calculation of $ALC_{animal}/ALC_{human}$ was based on 1-year exposure in rats and 50-year exposure in humans in order for PFOS to reach steady-state in both rats and humans. By linking the probabilistic EC10 (generated from Bayesian dose-response modeling) and reversed dosimetry equations (Eqs. (5) and (6)), the probabilistic HED based on human, animal and *in vitro* studies was derived. The estimated $C_{ss}$, AUC, ASC and ALC values were summarized in Table S1.

### 2.5. Risk characterization

#### 2.5.1. Conservative point of departure (POD) determination

To determine the conservative HEDs based on the comprehensive toxicity studies, we derived the threshold based on the probabilistic HEDs. Subsequently, a cumulative distribution function (CDF) of HEDs was constructed by assuming a Weibull distribution using the R package "fitdistrplus" (Delignette-Muller and Dutang, 2015). The threshold dose (TD) value was determined as the HED values at 5th percentile.

#### 2.5.2. Population-based risk assessment

The concept of probabilistic risk assessment has been previously reported in Chiu and Slob (2015). Several essential elements in probabilistic risk assessment include uncertainty, magnitude of effects, and population incidences (i.e. fraction of the population affected). To refine risk characterization, the exceedance probability profile that plots

the cumulative probability of exceedance versus the magnitude of effects was generated by integrating the distributions of exposure doses and corresponding effects estimated from the Bayesian dose-response model. The exceedance probability can be expressed as:

$$EP(x) = \int_0^1 D \cdot \int_x^\infty f_D(x)d(x)d(D) \quad (7)$$

where $D$ is probability density function (PDF) of internal dose metric of serum PFOS concentrations reported from the general populations in Asian, Australia, Europe and North America, respectively and fitted by lognormal distribution (Table S2). The $f_D(x)$ is the probability distribution of population having the certain incremental effects × at the probability of internal dose (D), which was estimated from the dose-response model $f(d;\theta)$. The exceedance probability EP (x) can be estimated by integrating the $\int_x^\infty f_D(x)d(x)$ over the exposure probability $D$, which represents the probability (i.e. fraction of population) having the effect of a particular endpoint that exceeds the effect of a certain magnitude $x$. Only the human epidemiological and ToxCast *in vitro* studies were included in the present population-based risk analysis; the animal experimental studies were excluded from this analysis to avoid extra uncertainty in the extrapolation from animals to humans.

## 3. Results

### 3.1. Hazard identification

In this study, we collected dose-response datasets in human epidemiological studies, animal *in vivo* toxicity studies and ToxCast *in vitro* assays for a comprehensive evaluation. Four human epidemiological studies with different populations were selected, including the C8 Health Project participants (Steenland et al., 2009), U.S. NHANES (National Health and Nutrition Examination Survey) participants (Nelson et al., 2010), Danish population (Eriksen et al., 2013), and Inuit population (Château-Degat et al., 2010). These studies reported the association between PFOS exposure and increased serum cholesterol in humans. In animals, six studies that showed increased liver weight by PFOS exposure in mice, rats, and monkeys were included in the dose-response analysis. In addition, the ToxCast *in vitro* assays related to PPAR activation, neurotoxicity, immunotoxicity, endocrine disruptors and cellular responses (including cytotoxicity, mitochondria, oxidative stress, DNA binding and cell cycle) were included in the *in vitro* dose-response model. The characteristics of these datasets were summarized in Tables 1 and 2. Additional description about these studies is available in the Supplementary Materials.

### 3.2. Dose-response modeling results

#### 3.2.1. Model parameters estimation

As listed in Tables 1 and 2, in total 34 datasets were included in the Bayesian dose-response analyses. The well-mixed Markov chains trace and probabilistic density plots (Figs. S2 and S3) for the population mean ($\mu_a$) and standard deviation ($\sigma_a$) of informative parameter "$a$" showed well convergences in all simulations (Scale Reduction Factors ($\widehat{R}$) ≤ 1.05 for all simulations). The posterior distributions of the median with 95% CI for the estimated model parameters ($a$, $b$, $c$) at the population level are shown in Table S3.

#### 3.2.2. Model evaluation and EC10 determination

The dose-response simulation results of these datasets are presented in Fig. 2. Most of the dose-response models fitted data points very well, with RAE of < 1 and Adj. $R^2$ of > 0.7 (Fig. 2). Two out of the 34 datasets ("Animal_1" and ToxCast_13") did not fit well, with the RAE of > 1 or the Adj. $R^2$ of < 0.5. Density plots of the distribution of the concentration or dose that caused 10% increase of the response over the control group (EC10) for each of the datasets are provided in Fig. 3. The median of EC10 of serum PFOS concentrations ranged from 0.19 to 7.13 ng/mL in human studies, 0.13 to 2.70 mg/kg/day in animal studies, and 1.62 to 109 μM in ToxCast *in vitro* studies (Table 3).

### 3.3. Determination of human equivalent dose (HED)

Table 3 showed the results of the estimated HEDs associated with calculated EC10 values across human epidemiological studies, animal *in vivo* studies and ToxCast *in vitro* assays. Using the previously developed multi-specie PBPK model (Chou and Lin, 2019), the ASC ($ASC_{human}$) and steady-state concentration ($C_{ss}$) in humans were determined to be 94,113 ng/mL and 13,571 μM on the basis of a daily oral intake of 1 mg/kg/day for 50 years (Table S1). The dose metric of $C_{ss}$ was used to calculate HEDs from *in vitro* assays, while the dose metric of ALC and ASC were used to calculate HEDs from animal and human studies, respectively. The estimated ALC values in monkeys, rats, and mice were 789,135, 172,059 and 462,833 ng/mL, respectively (Table S1). By the incorporating the ASC, ALC, and EC10 values into Eqs. (5) and (6), the associated HEDs were derived (Table 3).

### 3.4. HED variability across studies and threshold dose (TD) estimation

Inter-study variability in HEDs was visualized using boxplots across human, animal and ToxCast *in vitro* studies shown in Fig. 4. Overall, the median of HEDs was 1.78 μg/kg/day ($1.78 * 10^{-3}$ mg/kg/day) with 95% CI of 0.004–36.3 μg/kg/day, spanning over 5 orders of magnitude. The median of HEDs based animal and ToxCast *in vitro* studies were relatively similar (within 2 orders of magnitude difference), with a range of 1.41–54.3 and a 95% CI of 1.85–48.6 μg/kg/day in animal studies, as well as a range of 0.04–12.5 and a 95% CI of 0.11–8.55 μg/kg/day in ToxCast *in vitro* studies. On the other hand, the HEDs derived from human studies were generally lower than other studies, with a range of 0.0004–0.12 and a 95% CI of 0.0007–0.10 μg/kg/day (Fig. 4A).

To derive the TD values, the HEDs values across different endpoints in human, animal and ToxCast *in vitro* studies were fitted with Weibull distribution to construct the cumulative distribution function (CDF) with 95% confidence interval. The 5th percentile of HEDs (i.e. TD) with the corresponding 95% CI were determined as 21.5 (10.6–36.3) ng/kg/day (Fig. 4B). The lower bound of TD (10.6 ng/kg/day) was determined to be a conservative threshold dose which can be the basis in the determination of health-protective exposure limits.

### 3.5. Population-based risk characterization

The exceedance probability (% of population having equal to or greater than certain incremental changes of adverse effects) versus magnitude of percentage incremental changes of adverse effects for human serum cholesterol and *in vitro* studies associated with endpoints on PPAR, neurotoxicity, immunotoxicity, endocrine disruptors and cellular response is shown in Fig. 5 and Table 4. By linking the reported serum PFOS concentrations in the Asian, Australian, European and North American general populations, respectively (Table S2) with the constructed population dose-response models, the exceedance probabilities of different human populations due to PFOS exposure for different endpoints were estimated. The results showed that the incremental changes for different endpoints in the North American populations appeared to be slightly higher than Asian, Australian and European populations (Table 4). Fifty percentage of the North American population (EP = 0.5) had the incremental changes of 25.8% (95% CI: 14.4–36.4%) in increased serum cholesterol, 19.5% (95% CI: 18.0–23.4%) in PPAR activation, 7.92% (95% CI: 7.62–8.58%) in neurotoxicity, 9.17% (95%CI: 8.23–12.2%) in immunotoxicity, 10.7% (95% CI: 8.81–16.0%) in endocrine disruption, and 11.3% (95% CI: 10.1–14.5%) in cellular response (Fig. 5D1-D6, Table 4). None to minimal effects (< 20% critical effects) of neurotoxicity, immunotoxicity, endocrine disruption, and cellular response for 50% of

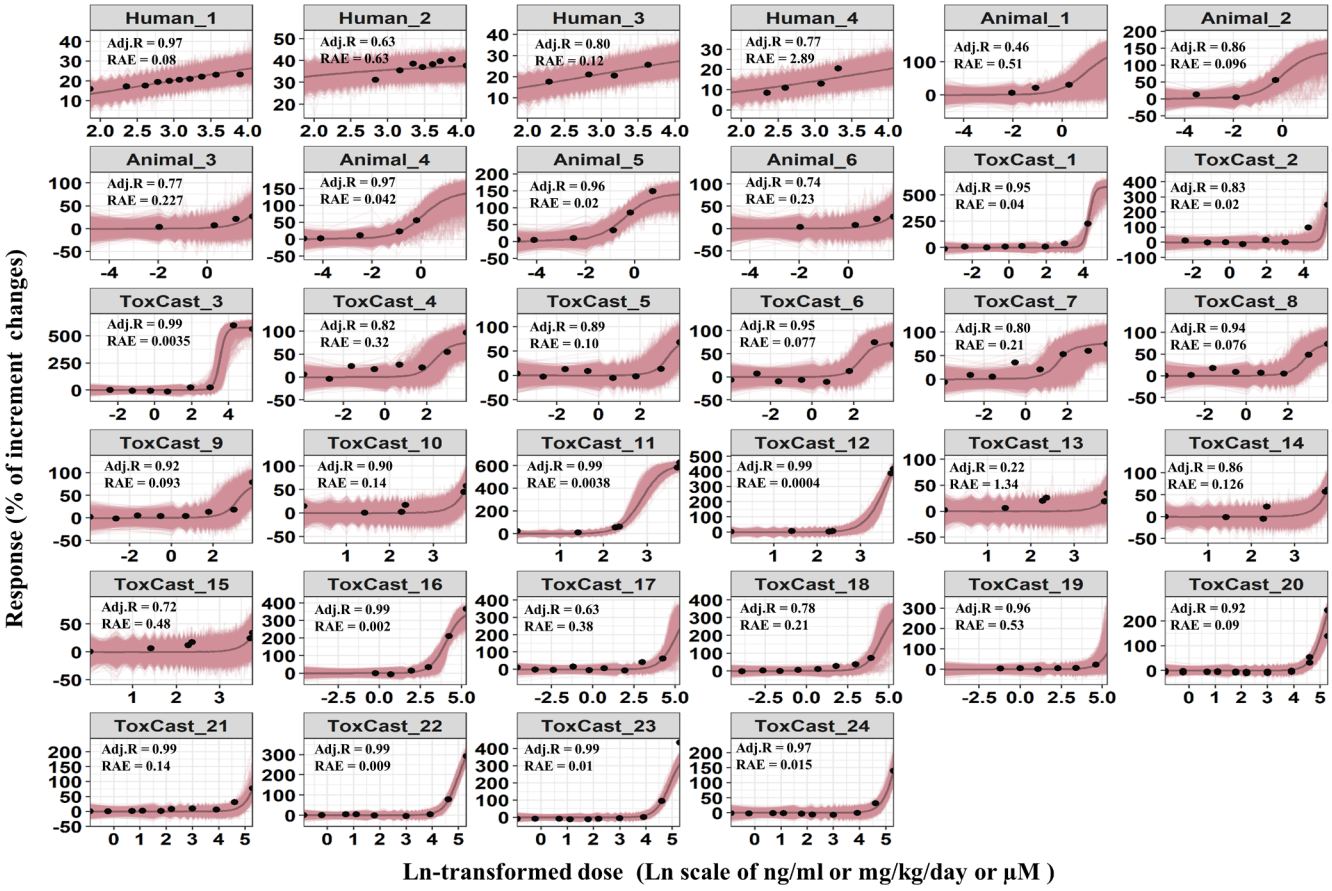


**Fig. 2.** Bayesian dose-response fitting results. The result for each of the 34 studies from human, animal, and ToxCast *in vitro* studies is shown as a separate panel. Dots represent the measured data points. Solid black line represents the population average (i.e., the median value) and pink lines represent individual simulated dose-response curves for the 5000 iterations. Adj.R: adjusted R square, RAE: relative absolute error. X axis represents the natural log-transformed (Ln) dose or concentration (Ln scale of μM or ng/ml or mg/kg/day).

human populations in all countries after exposure to the general environmental levels. It is also worth mentioning that high upper-bound effects of endocrine disruption (ER) and cellular response (CR) were estimated at the 10% of population (EP = 0.1) (i.e., sensitive population) in Asia (ER: 396% and CR: 497%), Australia (ER: 287% and CR: 311%), Europe (ER: 348% and CR: 433%) and North America (ER: 402% and CR: 502%) (Table 4). These significant increases might be because the general environmental exposure dose exceeds the threshold value that activates the relevant molecular initiating events.

## 4. Discussion

A major contribution of this study is the development of a probabilistic risk assessment framework that can integrate different types of toxicity studies with PBPK modeling to enhance the reliability in the determination of PODs and further improve risk assessment for PFOS. The Bayesian dose-response model can quantify the uncertainty and variability to derive the probabilistic POD based on a variety of toxicity datasets, including human epidemiology studies, animal *in vivo* studies, and ToxCast *in vitro* assays. Using the previously developed multi-species PBPK model can improve the toxicokinetic variability between species and convert the derived PODs into HEDs as the basis in the determination of RfDs for PFOS. As a demonstration, the present study framework was successfully applied to comprehensively estimate the population-based risk based on reported PFOS environmental exposure levels in the human general populations from different areas of the world to serve as a foundation for supporting better-informed risk management decisions of PFOS. This probabilistic framework can be extrapolated to other PFAS compounds to help regulatory agencies address risk assessment issues of this important family of environmental contaminants.

### 4.1. Comparison of PODs derived from in vivo and in vitro studies

Comprehensive dose-response evaluation integrating human epidemiological studies, animal experimental *in vivo* studies, and ToxCast *in vitro* assays provides important insights into PFOS-induced toxicity from molecular events to clinical phenotypes. Our results suggest that the ToxCast *in vitro* assays related to neurotoxicity and immunotoxicity are the most sensitive endpoints across the 24 selected *in vitro* assays (Fig. 4). When we compare the *in vitro* results with *in vivo* studies, we found that the derived PODs are consistent between *in vitro* and *in vivo* studies. The POD ranges derived from *in vitro* assays in the molecular events of PPAR activation, immunotoxicity, and cellular responses (oxidative stress and mitochondrial response) are similar to the values based on the endpoint of increased liver weight in rodent studies. This implies that there are plausible PFOS biological activity and hepatic toxicity at the similar dose ranges. Interestingly, our results are consistent with a previous study that showed transcriptional perturbation can occur at similar doses with apical responses in *in vivo* studies (Thomas et al., 2013).

### 4.2. Possible mode of action (MOA) of PFOS toxicity

The MOA of PFOS-induced hepatic toxicity in humans is not fully understood, but a growing number of studies in animals have been

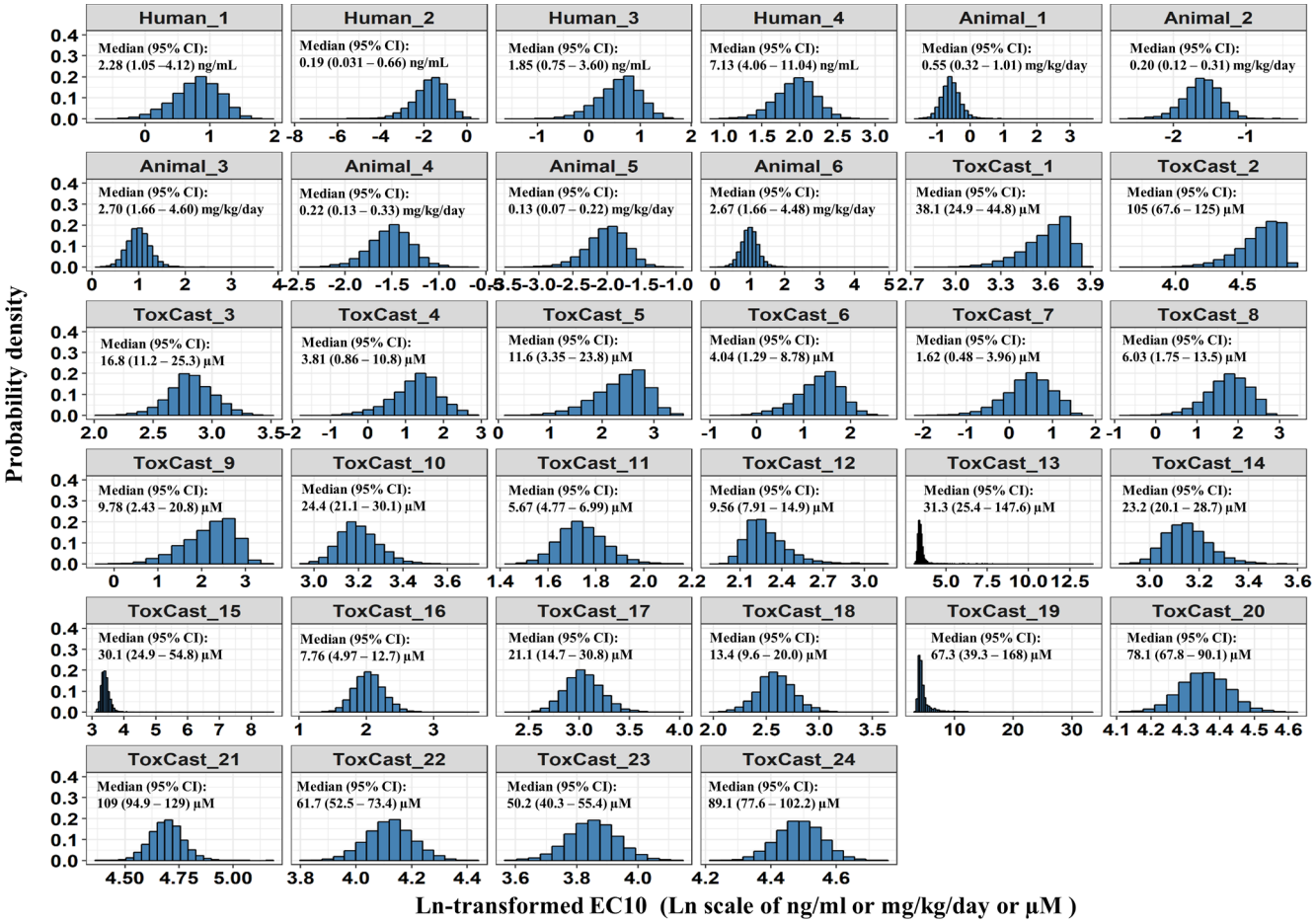


**Fig. 3.** Histogram plot of the natural log-transformed (Ln) EC10 values (Ln scale of µM or ng/ml or mg/kg/day) derived from the Bayesian dose-response analyses for the selected 34 datasets. The result of each dataset is shown as an individual panel.

trying to investigate MOA of PFOS. The leading hypothesis is that PFOS may interfere with mitochondrial beta-oxidation of fatty acids and subsequently affect the transcriptional activity of peroxisome proliferator-activated receptor alpha in liver, resulting in liver growth, proliferation of peroxisomes and induction of peroxisome beta-oxidation in rodents (Martin et al., 2007; Wan et al., 2012; Wang et al., 2015). Yet, in the present study, we found large differences in the range of POD values based on increased serum cholesterol observed in human studies compared with the ranges based on *in vivo* and *in vitro* studies. The mechanisms of PFOS-induced changes in plasma cholesterol levels in humans are unknown, but this effect is opposite to the observed effect in the rodent studies (Martin et al., 2007; Thibodeaux et al., 2003). Based on animal studies, PFOS has been suggested as a strong ligand of PPAR alpha and this binding can alter lipid metabolism to change serum lipid (Kennedy et al., 2004). On the other hand, PFOS and its related compounds have been shown to respond much less to PPAR alpha and its isoform in certain human cell lines than in rodents (Palmer et al., 1998; Takacs and Abbott, 2007). The differential response to PPAR alpha between species may partly explain the inconsistent ranges of derived-PODs between animal and human studies. Our results also suggest that the range of PODs based on elevated serum cholesterol in human studies is much lower than the POD range derived from ToxCast assays of PPAR activation. These results indicate that PPAR-independent mechanisms could be involved in PFOS-induced toxicity as well, leading to altered lipid metabolism at lower concentrations/doses.

### 4.3. Model-wise comparisons with BMDS and BBMD

The benchmark dose (BMD) method has been widely used to estimate the POD in the dose-response analysis for human health risk assessment. The BMD software (BMDS) developed by U.S. EPA has been accepted as a preferred tool for BMD estimation and used by risk assessors and scientists all over the world. More recently, a powerful web-based interface implementing Bayesian approach in BMD analysis (BBMD) was developed by Shao and Shapiro (2018). This tool allows users to estimate the probabilistic BMD and increases the reliability of dose-response analyses by incorporating the prior information. To better understand the results from the present Bayesian dose-response modeling, we compared the derived EC10 values from this study with the outputs from the BMDS and BBMD (Table S4, please refer to the Supplementary Materials for detailed methods). All the results of POD estimations from different tools based on the same datasets (34 studies in Tables 1 and 2) are summarized in Table S4. The ranges of median PODs for human studies were estimated to be 0.19–7.13, 0.27–5.96, and 6.13–19.8 ng/mL using the present approach, BMDS, and BBMD, respectively. For animal studies, the ranges of median PODs were estimated to be 0.13–2.70 (this study), 0.11–2.14 (BMDS), and 0.31–2.57 (BBMD) mg/kg/day. In the ToxCast *in vitro* studies, the ranges were 3.81–109, 0.96–94.23, and 0.69–74.5 µM based on the estimation from this study, BMDS, and BBMD, respectively. Despite of the differences of the methodology between our method and the BMD/BBMD tools, the similar ranges of derived PODs demonstrate the validity of the estimation of PODs of this study.

**Table 3**
Human equivalent doses (HEDs) for PFOS associated with EC10 derived from human epidemiological studies, animal *in vivo* studies, and ToxCast *in vitro* assays.

| Reference or ToxCast assay | EC10[a] (ng/mL or mg/kg/day or μM) | HED[b] (μg/kg/day) |
|---|---|---|
| **Human epidemiological studies** | | |
| Steenland et al. (2009) | 2.28 (1.05–4.12) | 0.02 (0.01–0.04) |
| Eriksen et al. (2013) | 0.19 (0.031–0.66) | 0.002 (0.0004–0.006) |
| Nelson et al. (2010) | 1.85 (0.75–3.60) | 0.019 (0.008–0.037) |
| Château-Degat et al. (2010) | 7.13 (4.06–11.04) | 0.07 (0.045–0.12) |
| **Animal *in vivo* studies** | | |
| Seacat et al. (2002) | 0.55 (0.32–1.01) | 30.3 (17.4–54.3) |
| Seacat et al. (2003) | 0.20 (0.12–0.31) | 2.39 (1.41–3.75) |
| Curran et al. (2008) | 2.70 (1.66–4.60) | 32.3 (19.7–54.1) |
| Dong et al.(2009) | 0.22 (0.13–0.33) | 7.07 (4.44–10.9) |
| Dong et al. (2011) | 0.13 (0.07–0.22) | 4.32 (2.21–7.29) |
| Lefebvre et al. (2008) | 2.67 (1.66–4.48) | 31.9 (19.6–53.5) |
| **ToxCast *in vitro* assays** | | |
| ATG_PPRE_CIS_up | 38.1 (24.9–44.8) | 2.81 (1.84–3.30) |
| ATG_PPARg_TRANS_up | 105 (67.6–125) | 7.80 (5.03–9.27) |
| NVS_GPCR_h5HT5A | 16.8 (11.2–25.3) | 1.24 (0.82–1.88) |
| NVS_GPCR_h5HT6 | 3.81 (0.86–10.8) | 0.28 (0.06–0.80) |
| NVS_GPCR_h5HT7 | 11.6 (3.35–23.8) | 0.87 (0.26–1.76) |
| NVS_GPCR_hAdoRA2a | 4.04 (1.29–8.78) | 0.29 (0.09–0.66) |
| NVS_GPCR_hAdra2C | 1.62 (0.48–3.96) | 0.12 (0.04–0.29) |
| NVS_GPCR_hAdrb1 | 6.03 (1.75–13.5) | 0.44 (0.13–0.98) |
| BSK_SAg_CD40_down | 9.78 (2.43–20.8) | 0.72 (0.18–1.52) |
| BSK_BE3C_IP10_down | 24.4 (21.1–30.1) | 1.79 (1.55–2.19) |
| BSK_BE3C_IL1a_down | 5.67 (4.77–6.99) | 0.42 (0.35–0.52) |
| BSK_LPS_IL8_up | 9.56 (7.91–14.9) | 0.70 (0.58–1.13) |
| BSK_3C_uPAR_down | 31.3 (25.4–147.6) | 2.29 (1.87–3.89) |
| BSK_CASM3C_VCAM1_down | 23.2 (20.1–28.7) | 1.71 (1.48–2.11) |
| NVS_NR_hAR | 30.1 (24.9–54.8) | 2.22 (1.83–3.33) |
| OT_ER_ERaERb_0480 | 7.76 (4.97–12.7) | 0.57 (0.36–0.95) |
| ATG_ERa_TRANS_up | 21.1 (14.7–30.8) | 1.55 (1.07–2.27) |
| ATG_ERE_CIS_up | 13.4 (9.6–20.0) | 9.85 (0.71–1.48) |
| NVS_NR_hTRa_Antagonist | 67.3 (39.3–168) | 4.97 (2.93–12.5) |
| APR_HepG2_CellLoss_24h_dn | 78.1 (67.8–90.1) | 5.74 (5.00–6.66) |
| APR_HepG2_MitoMass_24h_dn | 109 (94.9–129) | 8.07 (6.97–9.54) |
| APR_HepG2_OxidativeStress_24h_up | 61.7 (52.5–73.4) | 4.53 (3.86–5.39) |
| APR_HepG2_p53Act_24h_up | 50.2 (40.3–55.4) | 3.48 (2.97–4.06) |
| APR_HepG2_MitoticArrest_24h_up | 89.1 (77.6–102.2) | 6.57 (5.72–7.57) |

[a] The values represent median and 95% confidence interval (CI, i.e., 2.5th-97.5th percentiles) of EC10 (i.e., effective concentration resulting in 10% of changes); The unit of EC10 is ng/mL, mg/kg/day, μM in human, animal and ToxCast *in vitro* studies, respectively.

[b] The values represent median and 95% confidence interval (CI, i.e., 2.5th-97.5th percentiles) of HEDs (i.e., human equivalent doses) deriving from the corresponding EC10 values.

### 4.4. Model application for the derivation of RfD

Recently, the expert panels of National Research Council (NRC) (NRC, 2009) and World Health Organization International Program on Chemical Safety (WHO/IPCS) (WHO, 2017) proposed a probabilistic approach for dose-response analysis to unify across various endpoints from multiple sources. A probabilistic risk assessment approach integrating diverse datasets from different sources, species and endpoints may reduce some inherent uncertainty and limitations between and within studies/experiments. In line with the NRC and the WHO/IPCS guidelines, the major application of our developed probabilistic risk assessment framework is to determine the probabilistic POD values via a Bayesian dose-response model that accounts for the variability of data from different studies and species; and the resulting POD values can be converted into HEDs by using a well-validated multi-species PBPK model, which further reduces the interspecies uncertainty. Integrating the estimated HEDs derived from different PODs across human, *in vivo* and *in vitro* studies, the median of TD values with 95% CI was determined to be 21.5 (95% CI: 10.6–36.3) ng/kg/day. Using the estimated lower-bound TD values (10.6 ng/kg/day) and the uncertainty factor of 10 (only consider a factor of 10 to account for the intra-species variability because the interspecies variability of pharmacokinetics and pharmacodynamics has been considered in the PBPK model and Bayesian dose-response model, respectively), the estimated RfD value was 1.1 ng/kg/day. This RfD value is lower than the currently recommended value by U.S. EPA (20 ng/kg/day) (U.S. EPA, 2016), but it is close to the guidance values from EFSA (1.8 ng/kg/day) (EFSA, 2018) and German Federal Environment Agency (UBA) (0.4 ng/kg/day) (UBA, 2016). Overall, the estimated RfD based on the present study is within the range of RfDs recommended by different regulatory agencies (0.4–20 ng/kg/day). The differences in the RfDs between our study and the guidance values from different regulatory agencies are mainly due to different studies selected as the PODs to derived RfD. Since this study uses a unified probabilistic framework to integrate various types of toxicity data, the variability of PODs can be comprehensively characterized to improve the reliability in the determination of PODs. Moreover, the derived HED is lower than the HED estimated from our previously study (Chou and Lin, 2019) (e.g., 0.01 vs. 0.2 μg/kg/day). The difference is mainly because the present study framework incorporating the Bayesian dose-response model coupled with PBPK modeling can further reduce the toxicodynamic/toxicokinetic uncertainty in the derivation of HED. Thus, less uncertainty needs to be considered when deriving the RfD. Overall, this robust new approach can help support risk assessment of PFOS and its related compounds.

### 4.5. Population-based risk characterization

Compared with traditional risk assessment approach, probabilistic risk assessment can quantify a population-based risk estimation based on predicted chemical-induced toxicity effects and the uncertainty and variability of these effects. The NRC guideline on risk assessment has an emphasis on the population-based risk (NRC, 2009). Likewise, the WHO/IPCS guideline (WHO, 2017) emphasizes several essential elements on population risk assessment, especially the risk estimate associated with the population incidence of a specific magnitude of effect along with the derived confidence interval, which can replace the traditional risk characterization. Since the present dose-response analysis is based on a Bayesian approach, this probabilistic framework can be used to quantify the risk estimation in a population. Based on the WHO/IPCS guideline (WHO, 2017), our study characterizes the risk with two essential elements. First, the concept of harmful effects is quantified as a specific magnitude of effects with regard to the degree of harm (e.g., percentile). Second, the population dose-response model via Bayesian analysis allows us to estimate the probability or fraction of population which have the magnitude of effects or greater. By linking the reported serum PFOS concentration in the human general population from different areas of the world (Table S2) and the population dose-response model based on the endpoints of increased serum cholesterol, PPAR activation, neurotoxicity, immunotoxicity, endocrine disruption, and cellular response, a comprehensive population-based risk estimation for each endpoint was conducted in this study (Table 4). Based on the serum PFOS concentrations (Table S2) ranging from 0.05 to 214 ng/mL in the Asian population, 5 to 29.5 ng/mL in the Australian population, 0.06 to 92.5 ng/mL in the European population, and 0.4 to 1656 ng/mL in the North American general population, 50% of the population (EP = 0.5) has more than 10% incremental changes of increased serum cholesterol, PPAR activation, endocrine disruptions and cellular response due to environmental PFOS exposure. These results indicate that almost half of the general population may have at least 10% risk of these endpoints given the current environmental exposure levels (i.e., 0.04–1656 ng/mL plasma PFOS levels). This is not unexpected because numerous human epidemiological studies have reported the potential association between PFOS exposure and increased serum lipid levels in the human population, especially for PFOS-contaminated areas (Frisbee

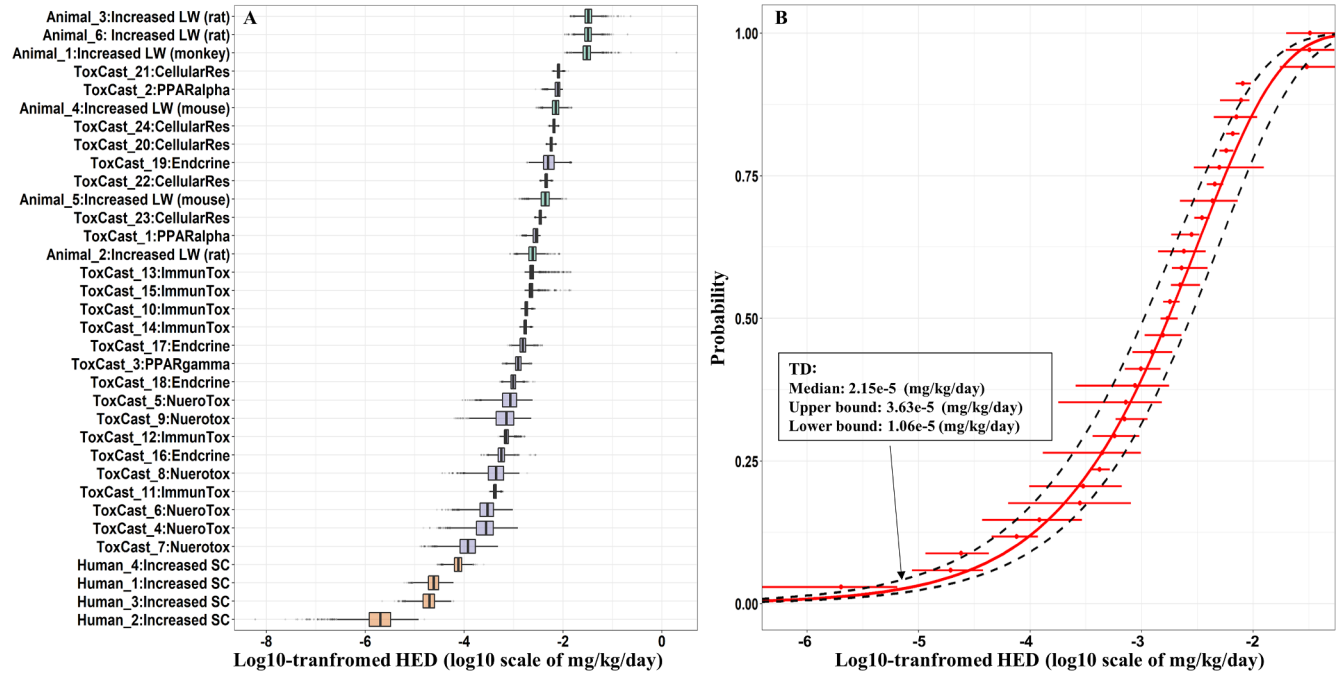


**Fig. 4.** Estimation of points of departure (PODs). (A) Comparison of PODs derived from human epidemiological, animal *in vivo*, and ToxCast *in vitro* studies; (B) Cumulative fitted Weibull distribution of PODs derived from human, animal *in vivo,* and ToxCast *in vitro* studies. In Fig. 4A, a total of 34 studies with specific endpoints are displayed as a box-and-whisker plot in the order from the lowest to the highest median dose. The vertical line depicts the median; the lower and upper edges of the box represent the 25th and 75th percentiles; and the whiskers represent the range of values 1.5 times the interquartile range below or above the 25th and 75th percentiles, respectively. In Fig. 4B, the solid line represents the median and the dash lines indicate the 95% CI. The horizontal line represents the range between highest and lowest POD values. *Abbreviations*: LW: liver weight; PPAR: PPAR activation; CelluarRes: Cellular response; Endocrine: endocrine disruption; ImmunoTox: Immunotoxicity; NeuroTox: neurotoxicity; SC: serum cholesterol.

et al., 2010; Steenland et al., 2009). Furthermore, PFOS-induced activation of PPAR and estrogen signaling pathway might subsequently trigger several cellular responses such as oxidative stress, cell proliferation and inflammation, etc., which supports our findings (Devchand et al., 1996; Jiang et al., 1998). In the risk estimation of the sensitive subpopulation, our results indicate that around 10% of the human population (EP = 0.1) has high incremental effects of endocrine disruption and cellular response. The results indicate that a certain fraction of the human population exposed to PFOS levels exceeding the threshold value that activates estrogen signaling pathway and subsequent cellular response. Overall, our results provide a probabilistic approach to characterize the possible risk estimates for different endpoints in the human population, and our results can support better-informed risk decisions.

### 4.6. Limitations

There are several limitations in this study. First, this study did not include all possible toxicity endpoints for PFOS in the dose-response analysis, thus, only the 34 critical datasets (including human epidemiological, animal *in vivo*, and ToxCast *in vitro* toxicity datasets) identified based on EFSA and U.S. EPA reports (EFSA, 2018; U.S. EPA, 2016) were considered in this study. Since hazard identification is a critical step of risk assessment, a systematic review and meta-analysis for PFOS toxicity is needed in the future to provide a more comprehensive risk assessment.

Second, the consideration of human epidemiological studies in the dose-response analysis has limitations on the assessing causality and co-exposure issues. The majority of human studies showing the association between PFOS or PFOA exposure and increase of serum lipid are cross-sectional studies, thus the results might not prove the causality. Yet, according to the EFSA report (EFSA, 2018), 26 epidemiological studies (including 16 cohorts) report the association between serum PFOS or PFOA and serum lipids based on all available human studies, and 16 studies in general populations show significant positive associations between PFOS and/or PFOA and total serum cholesterol. For PFOS, only one of these studies shows clear null results (Lin et al., 2011). Based on these human studies, EFSA concludes that it's likely there is a causal association between PFOS and increase of serum cholesterol (EFSA, 2018). Additionally, co-exposure confounding is common in epidemiological studies and it's difficult to disentangle the effect of PFOS from PFOA or other PFAS compounds. However, based on the current EFSA's report (EFSA, 2018), the EFSA expert panel recognizes this limitation and concludes: "It is likely that adjustment for PFOA (and maybe other PFASs) would result in somewhat higher BMDL5 values and corresponding daily intake rates". Accordingly, our estimated EC10 and HED might be more conservative than the values by the adjustment of the effects from other PFAS compounds.

Third, the incorporation of ToxCast *in vitro* datasets in the dose-response analysis has a variety of inherent limitations and faces multiple challenges. For IVIVE, the underlying hypothesis is that the average plasma concentration or steady-state plasma concentration equivalent to or higher than *in vitro* POD would produce responses *in vivo* (Rotroff et al., 2010; Wetmore et al., 2015, 2012). However, it is known that perturbations of biological pathways *in vitro* do not necessarily result in adverse effects *in vivo* (Krewski et al., 2019). Also, this assumption implies that the *in vitro* system has equal or similar exposure duration or biological time scale to the *in vivo* studies despite the fact that *in vitro* assays are often short-term duration (e.g., hours or days) as opposed to the exposure duration in animals and humans (e.g., months or years). In addition, the nominal concentrations in the *in vitro* systems are typically used in the toxicity testing via the IVIVE approach based on the ToxCast data (Wetmore et al., 2015, 2013, 2012). However, the effective free chemical concentration (i.e., unbound concentration) in the *in vitro* assays that triggers a response might differ from the nominal concentration because of factors such as the

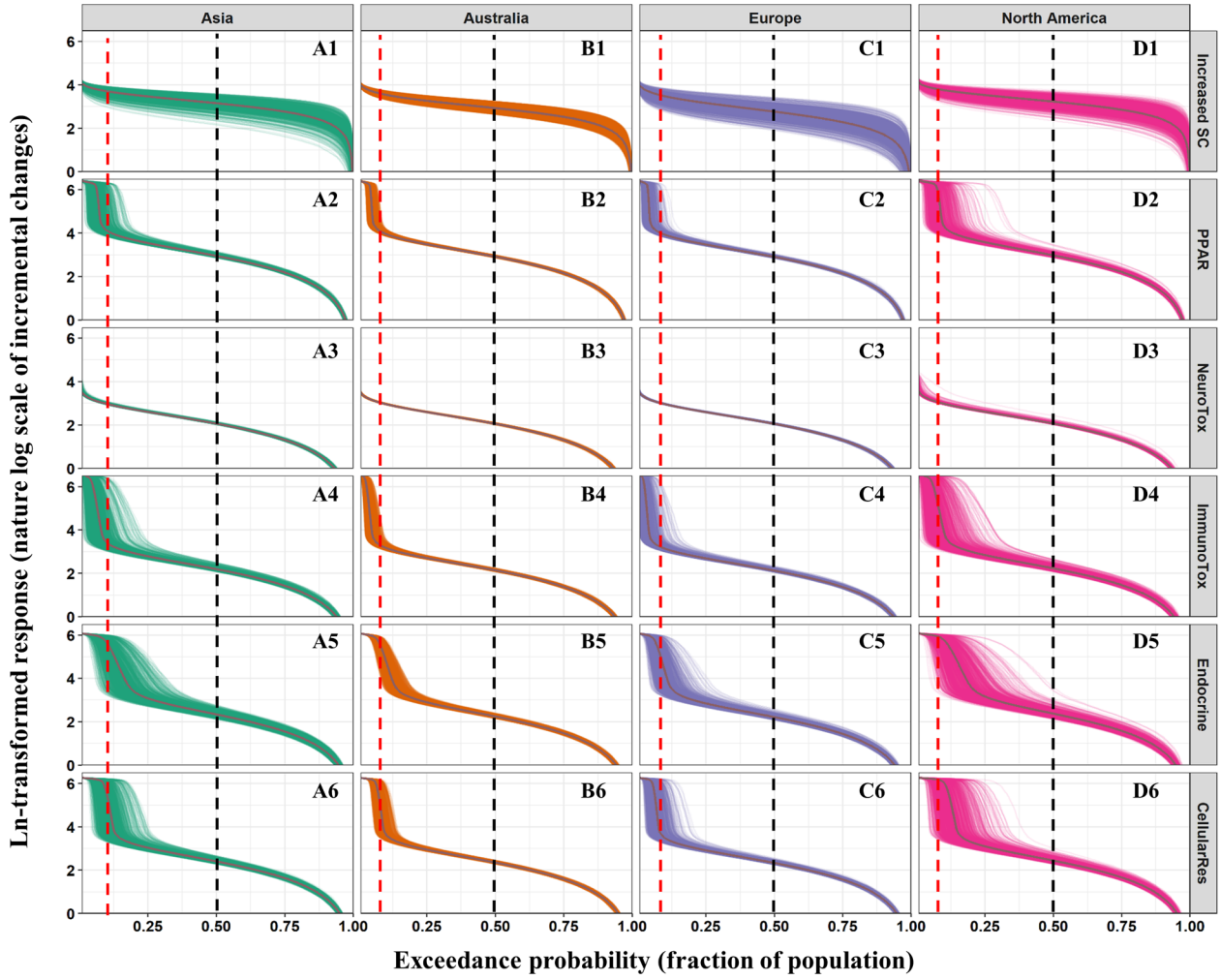


**Fig. 5.** Exceedance probability profiles across human and ToxCast *in vitro* studies for endpoints of (A1, B1, C1, D1) increased serum cholesterol (human), (A2, B2, C2, D2) PPAR activation (*in vitro*), (A3, B3, C3, D3) neurotoxicity (*in vitro*), (A4, B4, C4, D4) immunotoxicity, (A5, B5, C5, D5) endocrine disruption, and (A6, B6, C6, D6) cellular response in Asian (A1-A6), Australian (B1-B6), European (C1-C6) and North American populations (D1-D6). Solid pink bold curve in each panel represents the population average curve; and the solid light curves in each panel represent individual simulated risk curves for 1000 iterations. Red vertical dashed line represents the exceedance probability (EP) of 10% (EP = 0.1) and black vertical dashed line represents the EP of 50% (EP = 0.5). *Abbreviations*: SC: serum cholesterol; PPAR: PPAR activation; NeuroTox: neurotoxicity; ImmunoTox: Immunotoxicity; Endocrine: endocrine disruption; CellularRes: Cellular response.

composition of the cell media and binding of the chemicals to plastic well or ingredients (Blaauboer, 2010). The above-mentioned challenges might lead to uncertainty in our *in vitro* POD estimation and need to be addressed in the future. In addition, the cellular response in the *in vitro* systems might be very different from the response of cells *in vivo* which can experience dynamic or relatively constant chemical concentrations depending on the real-world exposure scenarios and physiological clearance rates. Thus, it is difficult to directly link *in vitro* activity to adverse outcomes/disease endpoints and there is an inherent limitation to correlate the bioactivity in *in vitro* systems with the response or biomarkers *in vivo*. These limitations and challenges related to the use of *in vitro* assays in risk assessment are further discussed in the recent report on the vision, progress, and challenges of the Toxicity Testing in the 21st Century (Tox21) program (Krewski et al., 2019).

To better link *in vitro* assays to *in vivo* toxicity and risk assessment, computational models that can mechanistically describe chemical toxicokinetics and toxicodynamics and can correlate *in vitro* activity with *in vivo* toxicity are needed. For example, several PBPK models have been expanded to include a toxicodynamic component to become biologically based dose-response (BBDR) models to interpret dose-response data at the cellular and molecular levels based on the biological basis and to link external exposure with an adverse effect. Examples include the carcinogenic effects of formaldehyde (Conolly et al., 2004, 2003) and an evaluation of a hypothesized MOA for the disruption of hypothalamic–pituitary–thyroid axis homeostasis by perchlorate (McLanahan et al., 2009). BBDR models can provide a probabilistic prediction of an adverse outcome in humans by a function of quantitative biological events (e.g., production rates of hormones, cell division rates) involved in the response. A PBPK model can provide a linkage to express the exposure in the target organ as a function of external response. Thus, further studies are needed to develop BBDR models that will provide a useful framework for integrating available dose-response data from *in vitro* and *in vivo* studies, evaluating the possible MOA from molecular levels to adverse outcomes for PFOS and other PFAS compounds.

Fourth, this study was not designed to compare different dose-response models, thus, only the Hill dose-response model was considered in this study. This was because the Hill model can directly parameterize the efficacy and potency with the Emax (maximal response) and EC50 (concentration at the half maximal response), it is frequently used in estimating monotonic dose-response curves and recommended by EFSA and U.S. EPA for benchmark dose estimation (EFSA, 2017; U.S. EPA, 2012). Also, the log-form Hill model has been successfully implemented to fit the ToxCast *in vitro* data (Tice et al., 2013; Watt and Judson,

**Table 4**
Exceedance probability (median with 95% CI) of PFOS-induced adverse effects based on human and ToxCast studies in Asian, Australian, European and North American population.

| Exceedance[a] probability (EP) | Critical effects[b] (% of incremental changes) | | | | | |
|---|---|---|---|---|---|---|
| | Increased SC | PPAR | NeuroTox | ImmunoTox | ER | CR |
| Asia | | | | | | |
| EP = 0.1 | 38.8 (26.3–48.9) | 59.2 (48.1–548) | 19.5 (18.9–20.7) | 28.5 (21.6–574) | 243 (31.8–396) | 168 (28.7–497) |
| EP = 0.5 | 22.9 (12.9–33.6) | 19.1 (17.9–22.1) | 7.88 (7.58–8.31) | 8.94 (8.15–11.3) | 10.2 (8.67–14.1) | 11.0 (9.98–13.6) |
| EP = 0.9 | 10.8 (4.80–19.5) | 3.49 (3.14–3.97) | 1.46 (1.33–1.61) | 1.63 (1.45–1.96) | 1.83 (1.54–2.36) | 2.01 (1.78–2.37) |
| Australia | | | | | | |
| EP = 0.1 | 33.8 (28.1–40.6) | 52.4 (48.5–62.9) | 19.4 (18.9–19.9) | 23.9 (21.6–30.8) | 109 (35.4–287) | 36.2 (20.1–311) |
| EP = 0.5 | 18.5 (14.2–24.6) | 18.5 (17.8–19.6) | 7.82 (7.56–8.01) | 8.54 (8.12–9.12) | 9.44 (8.79–10.6) | 10.5 (9.94–11.4) |
| EP = 0.9 | 7.88 (5.41–11.9) | 3.41 (3.12–3.72) | 1.45 (1.33–1.59) | 1.58 (1.43–1.73) | 1.71 (1.54–1.92) | 1.93 (1.75–2.15) |
| Europe | | | | | | |
| EP = 0.1 | 30.6 (18.8–42.2) | 50.3 (45.9–77.3) | 19.4 (18.8–19.9) | 22.6 (20.4–48.8) | 59.6 (24.5–348) | 31.3 (25.8–433) |
| EP = 0.5 | 16.0 (8.31–26.3) | 18.4 (17.5–19.9) | 7.82 (7.56–8.07) | 8.39 (7.96–9.34) | 9.12 (8.27–11.3) | 10.3 (9.65–11.7) |
| EP = 0.9 | 6.42 (2.50–13.3) | 3.38 (3.09–3.72) | 1.45 (1.33–1.58) | 1.55 (1.40–1.74) | 1.66 (1.46–2.00) | 1.89 (1.72–2.13) |
| North America | | | | | | |
| EP = 0.1 | 41.7 (28.4–51.3) | 65.1 (49.2–564) | 19.7 (18.9–21.9) | 33.6 (21.8–616) | 305 (35.3–402) | 330 (29.5–502) |
| EP = 0.5 | 25.8 (14.4–36.4) | 19.5 (18.0–23.4) | 7.92 (7.62–8.58) | 9.17 (8.23–12.2) | 10.7 (8.81–16.0) | 11.3 (10.1–14.5) |
| EP = 0.9 | 12.9 (5.45–22.1) | 3.56 (3.18–4.18) | 1.48 (1.35–1.65) | 1.68 (1.47–2.09) | 1.91 (1.57–2.57) | 2.05 (1.79–2.54) |

[a] Exceedance probability (EP) indicate the percentage of population with effects equal to or greater than the magnitude of the critical effects (e.g., EP = 0.1/0.5/0.9 represent the 10/50/90% of population with certain effects equal to or greater than the magnitude of critical effects).
[b] The critical effects indicate the percentage of incremental changes that calculated from human and in ToxCast *in vitro* studies based on the endpoints of increased serum cholesterol (SC), PPAR pathways activation (PPAR), neurotoxicity (NeuroTox), Immunotoxicity (ImmunoTox), endocrine disruption (ER) and cellular response (CR).

2018). It is recognized that sometimes the Hill model may not the best dose-response model to describe dose-response data. In this study, the Hill model and its log-transformed equation failed to fit two out of the 34 datasets (i.e., adjusted R square lower than 0.5). The results from these two datasets may cause some uncertainty in the identification of POD values. Additional studies might be needed to explore different models (e.g., linear, exponential, and logistic models).

Fifth, the magnitude of effects in the dose-response analysis was standardized to incremental change compared to the control group without further considering the differential severities of different endpoints. For instance, 10% incremental change of the *in vitro* toxicity endpoints (e.g., gene expression or cellular response) has a different severity compared with that of *in vivo* endpoints (e.g., increased liver weight) and human endpoints (e.g., increased serum cholesterol). The variation in the severity of different endpoints might also impact risk estimation and decision. However, the differences in the severity of different endpoints can be accommodated by specifying different levels based on MOAs or adverse outcome pathways to provide a more complete risk characterization (Cote et al., 2016), which warrants further studies. In addition, some specific *in vitro* responses (e.g., estrogen signaling pathway) are sex-dependent. Future studies are needed to refine this approach further by evaluating sex-specific differences on the predicted outcomes. Also, this study does not include the reproductive/developmental toxicity as the endpoint for the dose-response analysis because our PBPK model is in adults. However, the developmental effects for the fetus, neonate, and infant are considered to be the most sensitive toxicity endpoints for PFOS (U.S. EPA, 2016). Future studies are needed to extend the present PBPK model from the adulthood to other life stages, particularly in gestational and lactational periods. Finally, the present study uses a subchronic-to-chronic uncertainty factor of 1-fold due to lack of chronic study data that are suitable for dose-response analysis of the selected endpoint of increased liver weight. Although this uncertainty factor has been used by other regulatory agencies and is well justified in the recent U.S. EPA report (Dong et al., 2017; U.S. EPA, 2016), this remains one uncertainty of this study and should be addressed when relevant chronic study data are available in the future.

## 5. Conclusions

In this study, we developed and applied a probabilistic risk assessment approach to improve the derivation of RfDs and to further inform risk assessment in the human population using PFOS as a case study. Our results suggested that the model-derived *in vitro* PODs are similar to the POD values derived from animal *in vivo* studies, but they are quite different from the PODs derived from human studies. The estimated RfDs from this study is lower than the guidance value recommended by U.S. EPA, but it is close to the guidance values suggested by EFSA and UBA. In addition, there may be 50% of population in all studied countries having more than 10% incremental changes of evaluated serum cholesterol and PPAR activation based on reported serum PFOS levels in the different areas of the world. Moreover, there may be a small percentage (10%) of the general population that may be highly sensitive to PFOS toxicity. Overall, our results provide insights into risk assessment of PFOS and the present probabilistic risk assessment framework can be used for other PFAS compounds to facilitate the risk decisions of this important family of environmental contaminants.

## 6. Author statement

Zhoumeng Lin and Wei-Chun Chou conceived and designed the study. Wei-Chun Chou collected and extracted all the experimental data from the literature and the ToxCast database. Wei-Chun Chou wrote all the model codes, developed the dose-response model, implemented the probabilistic human health risk assessment framework, and analyzed all the data. Zhoumeng Lin checked every line of the model codes, corrected the model codes, re-ran the model simulations, and re-produced the results. Wei-Chun Chou drafted the manuscript. Zhoumeng Lin mentored and coordinated the project, and comprehensively revised the manuscript. Both authors have read and approved the final manuscript.

## Declaration of Competing Interest

The authors declare they have no actual or potential competing financial interests.

## Acknowledgments

This study was supported by Kansas State University College of Veterinary Medicine New Faculty Startup funds.

## Appendix A. Supplementary material

Supplementary data to this article can be found online at https://doi.org/10.1016/j.envint.2020.105581.

## References

Andersen, M.E., Sarangapani, R., Frederick, C., Kimbell, J., 2002. Dosimetric adjustment factors for methyl methacrylate derived from a steady-state analysis of a physiologically based clearance-extraction model. Inhal. Toxicol. 11, 899–926. https://doi.org/10.1080/089583799196709.

Butenhoff, J.L., Ehresman, D.J., Chang, S.C., Parker, G.A., Stump, D.G., 2009. Gestational and lactational exposure to potassium perfluorooctanesulfonate (K+PFOS) in rats: Developmental neurotoxicity. Reprod. Toxicol. 27, 319–330. https://doi.org/10.1016/j.reprotox.2008.12.010.

Butenhoff, J.L., Chang, S.C., Olsen, G.W., Thomford, P.J., 2012. Chronic dietary toxicity and carcinogenicity study with potassium perfluorooctanesulfonate in Sprague Dawley rats. Toxicology 293, 1–15. https://doi.org/10.1016/j.tox.2012.01.003.

Blaauboer, B.J., 2010. Biokinetic modeling and in vitro-in vivo extrapolations. J. Toxicol. Environ. Heal. - Part B Crit. Rev. 13 (2–4), 242–252. https://doi.org/10.1080/10937404.2010.483940.

Calafat, A.M., Wong, L.Y., Kuklenyik, Z., Reidy, J.A., Needham, L.L., 2007. Polyfluoroalkyl Chemicals in the U.S. Population: data from the National Health and Nutrition Examination Survey (NHANES) 2003–2004 and comparisons with NHANES 1999–2000. Environ. Health Perspect. 115, 1596–1602. https://doi.org/10.1289/ehp.10598.

Carpenter, B., Gelman, A., Hoffman, M.D., Lee, D., Goodrich, B., Betancourt, M., Brubaker, M., Guo, J., Li, P., Riddell, A., 2017. Stan: a probabilistic programming language. J. Stat. Softw. 76, 1–32. https://doi.org/10.18637/jss.v076.i01.

Château-Degat, M.-L., Pereg, D., Dallaire, R., Ayotte, P., Dery, S., Dewailly, É., 2010. Effects of perfluorooctanesulfonate exposure on plasma lipid levels in the Inuit population of Nunavik (Northern Quebec). Environ. Res. 110, 710–717. https://doi.org/10.1016/J.ENVRES.2010.07.003.

Cheng, Y.H., Riviere, J.E., Monteiro-Riviere, N.A., Lin, Z., 2018. Probabilistic risk assessment of gold nanoparticles after intravenous administration by integrating in vitro and in vivo toxicity with physiologically based pharmacokinetic modeling. Nanotoxicology 12, 453–469. https://doi.org/10.1080/17435390.2018.1459922.

Chiu, W., Wright, F.A., Rusyn, I., 2017. A tiered, Bayesian approach to estimating population variability for regulatory decision-making. ALTEX 34, 377–388. https://doi.org/10.14573/altex.1608251.

Chiu, W., Slob, W., 2015. A unified probabilistic framework for dose–response assessment of human health effects. Environ. Health Perspect. 123, 1241–1254. https://doi.org/10.1289/ehp.1409385.

Chou, W.C., Lin, Z., 2019. Bayesian evaluation of a physiologically based pharmacokinetic (PBPK) model for perfluorooctane sulfonate (PFOS) to characterize the interspecies uncertainty between mice, rats, monkeys, and humans: development and performance verification. Environ. Int. 129, 408–422. https://doi.org/10.1016/j.envint.2019.03.058.

Conolly, R.B., Kimbell, J.S., Janszen, D., Schlosser, P.M., Kalisak, D., Preston, J., Miller, F.J., 2004. Human respiratory tract cancer risks of inhaled formaldehyde: dose-response predictions derived from biologically-motivated computational modeling of a combined rodent and human dataset. Toxicol. Sci. 82, 279–296. https://doi.org/10.1093/toxsci/kfh223.

Conolly, R.B., Kimbell, J.S., Janszen, D., Schlosser, P.M., Kalisak, D., Preston, J., Miller, F.J., 2003. Biologically motivated computational modeling of formaldehyde carcinogenicity in the F344 rat. Sci. Toxicol. https://doi.org/10.1093/toxsci/kfg182.

Cote, I., Andersen, M.E., Ankley, G.T., Barone, S., Birnbaum, L.S., Boekelheide, K., Bois, F.Y., Burgoon, L.D., Chiu, W.A., Crawford-Brown, D., Crofton, K.M., DeVito, M., Devlin, R.B., Edwards, S.W., Guyton, K.Z., Hattis, D., Judson, R.S., Knight, D., Krewski, D., Lambert, J., Maull, E.A., Mendrick, D., Paoli, G.M., Patel, C.J., Perkins, E.J., Poje, G., Portier, C.J., Rusyn, I., Schulte, P.A., Simeonov, A., Smith, M.T., Thayer, K.A., Thomas, R.R.S., Thomas, R.R.S., Tice, R.R., Vandenberg, J.J., Villeneuve, D.L., Wesselkamper, S., Whelan, M., Whittaker, C., White, R., Xia, M., Yauk, C., Zeise, L., Zhao, J., DeWoskin, R.S., 2016. The next generation of risk assessment multi-year study—highlights of findings, applications to risk assessment, and future directions. Environ. Health Perspect. 124, 1671–1682. https://doi.org/10.1289/EHP233.

Curran, I., Hierlihy, S.L., Liston, V., Pantazopoulos, P., Nunnikhoven, A., Tittlemier, S., Barker, M., Trick, K., Bondy, G., 2008. Altered fatty acid homeostasis and related toxicologic sequelae in rats exposed to dietary potassium perfluorooctanesulfonate (PFOS). J. Toxicol. Environ. Heal. - Part A Curr. Issues 71, 1526–1541. https://doi.org/10.1080/15287390802361763.

Delignette-Muller, M.L., Dutang, C., 2015. fitdistrplus: an R package for fitting distributions. J. Stat. Softw. 64, 1–34. https://doi.org/10.18637/jss.v064.i04.

Devchand, P.R., Keller, H., Peters, J.M., Vazquez, M., Gonzalez, F.J., Wahli, W., 1996. The PPARα–leukotriene B4 pathway to inflammation control. Nature 384, 39–43. https://doi.org/10.1038/384039a0.

Dong, G.H., Zhang, Y.H., Zheng, L., Liu, W., Jin, Y.-H., He, Q.C., 2009. Chronic effects of perfluorooctanesulfonate exposure on immunotoxicity in adult male C57BL/6 mice. Arch. Toxicol. 83, 805–815. https://doi.org/10.1007/s00204-009-0424-0.

Dong, G.H., Liu, M.M., Wang, D., Zheng, L., Liang, Z.F., Jin, Y.H., 2011. Sub-chronic effect of perfluorooctanesulfonate (PFOS) on the balance of type 1 and type 2 cytokine in adult C57BL6 mice. Toxicol. Arch. https://doi.org/10.1007/s00204-011-0661-x.

Dong, Z., Bahar, M.M., Jit, J., Kennedy, B., Priestly, B., Ng, J., Lamb, D., Liu, Y., Duan, L., Naidu, R., 2017. Issues raised by the reference doses for perfluorooctane sulfonate and perfluorooctanoic acid. Environ. Int. 105, 86–94. https://doi.org/10.1016/J.ENVINT.2017.05.006.

EFSA, 2008. Perfluorooctane Sulfonate (PFOS), Perfluorooctanoic Acid (PFOA) and their salts scientific opinion of the panel on contaminants in the food chain. Parma, European Food Safety Authority; Available: https://doi.org/10.2903/j.efsa.2008.653 [accessed 1 August 2019].

EFSA, 2017. Update: use of the benchmark dose approach in risk assessment. Parma, European Food Safety Authority; Available: https://doi.org/10.2903/j.efsa.2017.4658 [accessed 1 August 2019].

EFSA, 2018. Risk to human health related to the presence of perfluorooctane sulfonic acid and perfluorooctanoic acid in food. Parma, European Food Safety Authority; Available: https://doi.org/10.2903/j.efsa.2018.5194 [accessed 1 August 2019].

Eriksen, K.T., Raaschou-Nielsen, O., McLaughlin, J.K., Lipworth, L., Tjønneland, A., Overvad, K., Sørensen, M., 2013. Association between plasma PFOA and PFOS levels and total cholesterol in a middle-aged Danish population. PLoS ONE 8, e56969. https://doi.org/10.1371/journal.pone.0056969.

FDA, 2011. Update on perfluorinated grease-proofing agents. Available: https://www.fda.gov/food/inventory-effective-food-contact-substance-fcs-notifications/update-perfluorinated-grease-proofing-agents.

Frisbee, S.J., Shankar, A., Knox, S.S., Steenland, K., Savitz, D.A., Fletcher, T., Ducatman, A.M., 2010. Perfluorooctanoic acid, perfluorooctanesulfonate, and serum lipids in children and adolescents: results from the C8 health project. Pediatr. Adolesc. Med. Arch. https://doi.org/10.1001/archpediatrics.2010.163.

Geiger, S.D., Xiao, J., Ducatman, A., Frisbee, S., Innes, K., Shankar, A., 2014. The association between PFOA, PFOS and serum lipid levels in adolescents. Chemosphere 98, 78–83. https://doi.org/10.1016/j.chemosphere.2013.10.005.

Gelman, A., 2006. Prior distributions for variance parameters in hierarchical models (comment on article by Browne and Draper). Bayesian Anal. 1, 515–534. https://doi.org/10.1214/06-BA117A.

Grundy, S.M., Stone, N.J., Bailey, A.L., Beam, C., Birtcher, K.K., Blumenthal, R.S., Braun, L.T., de Ferranti, S., Faiella-Tommasino, J., Forman, D.E., Goldberg, R., Heidenreich, P.A., Hlatky, M.A., Jones, D.W., Lloyd-Jones, D., Lopez-Pajares, N., Ndumele, C.E., Orringer, C.E., Peralta, C.A., Saseen, J.J., Smith, S.C., Sperling, L., Virani, S.S., Yeboah, J., 2019. 2018 AHA/ACC/AACVPR/AAPA/ABC/ACPM/ADA/AGS/APhA/ASPC/NLA/PCNA guideline on the management of blood cholesterol: a report of the American college of cardiology/American heart association task force on clinical practice guidelines. Circulation 139. https://doi.org/10.1161/CIR.0000000000000625.

Haber, L.T., Dourson, M.L., Allen, B.C., Hertzberg, R.C., Parker, A., Vincent, M.J., Maier, A., Boobis, A.R., 2018. Benchmark dose (BMD) modeling: current practice, issues, and challenges. Crit. Rev. Toxicol. 48, 387–415. https://doi.org/10.1080/10408444.2018.1430121.

Hu, X.C., Andrews, D.Q., Lindstrom, A.B., Bruton, T.A., Schaider, L.A., Grandjean, P., Lohmann, R., Carignan, C.C., Blum, A., Balan, S.A., Higgins, C.P., Sunderland, E.M., 2016. Detection of Poly- and Perfluoroalkyl Substances (PFASs) in U.S. drinking water linked to industrial sites, military fire training areas, and wastewater treatment plants. Environ. Sci. Technol. Lett. 3, 344–350. https://doi.org/10.1021/acs.estlett.6b00260.

Jiang, C., Ting, A.T., Seed, B., 1998. PPAR-γ agonists inhibit production of monocyte inflammatory cytokines. Nature 391, 82–86. https://doi.org/10.1038/34184.

Kennedy, G.L., Butenhoff, J.L., Olsen, G.W., O'Connor, J.C., Seacat, A.M., Perkins, R.G., Biegel, L.B., Murphy, S.R., Farrar, D.G., 2004. The toxicology of perfluorooctanoate. Crit. Rev. Toxicol. 34, 351–384. https://doi.org/10.1080/10408440490464705.

Krewski, D., Andersen, M.E., Tyshenko, M.G., Krishnan, K., Hartung, T., Boekelheide, K., Wambaugh, J.F., Jones, D., Whelan, M., Thomas, R., Yauk, C., Barton-Maclaren, T., Cote, I., 2019. Toxicity testing in the 21st century: progress in the past decade and future perspectives. Toxicol. Arch. https://doi.org/10.1007/s00204-019-02613-4.

Kavlock, R.J., Austin, C.P., Tice, R.R., 2019. US vision for toxicity testing in the 21st Century. In: The History of Alternative Test Methods in Toxicology. Elsevier, pp. 129–136. doi: 10.1016/b978-0-12-813697-3.00016-0.

Lau, C., Thibodeaux, J.R., Hanson, R.G., Rogers, J.M., Grey, B.E., Stanton, M.E., Buttenhoff, J.L., Stevenson, L.A., 2003. Exposure to perfluorooctane sulfonate during pregnancy in rat and mouse. II: Postnatal evaluation. Toxicol. Sci. https://doi.org/10.1093/toxsci/kfg122.

Lefebvre, D.E., Curran, I., Armstrong, C., Coady, L., Parenteau, M., Liston, V., Barker, M., Aziz, S., Rutherford, K., Bellon-Gagnon, P., Shenton, J., Mehta, R., Bondy, G., 2008. Immunomodulatory effects of dietary potassium perfluorooctane sulfonate (PFOS) exposure in adult Sprague-Dawley rats. J. Toxicol. Environ. Heal. - Part A Curr. Issues. https://doi.org/10.1080/15287390802391943.

Lin, Z., Monteiro-Riviere, N.A., Kannan, R., Riviere, J.E., 2016. A computational framework for interspecies pharmacokinetics, exposure and toxicity assessment of gold nanoparticles. Nanomedicine 11, 107–119. https://doi.org/10.2217/nnm.15.177.

Lin, C.Y., Wen, L.L., Lin, L.Y., Wen, T.W., Lien, G.W., Chen, C.Y., et al., 2011. Associations between levels of serum perfluorinated chemicals and adiponectin in a young hypertension cohort in Taiwan. Environ Sci Technol. 45, 10691–10698. https://doi.org/10.1021/es201964x.

Luebker, D.J., Case, M.T., York, R.G., Moore, J.A., Hansen, K.J., Butenhoff, J.L., 2005a. Two-generation reproduction and cross-foster studies of perfluorooctanesulfonate

(PFOS) in rats. Toxicology 215, 126–148. https://doi.org/10.1016/J.TOX.2005.07.018.
Luebker, D.J., York, R.G., Hansen, K.J., Moore, J.A., Butenhoff, J.L., 2005b. Neonatal mortality from in utero exposure to perfluorooctanesulfonate (PFOS) in Sprague-Dawley rats: Dose-response, and biochemical and pharamacokinetic parameters. Toxicology 215, 149–169. https://doi.org/10.1016/j.tox.2005.07.019.
Lyons, M.A., Yang, R.S.H., Mayeno, A.N., Reisfeld, B., 2008. Computational toxicology of chloroform: reverse dosimetry using Bayesian inference, Markov Chain Monte Carlo simulation, and human biomonitoring data. Environ. Health Perspect. 116, 1040–1046. https://doi.org/10.1289/ehp.11079.
Mamsen, L.S., Björvang, R.D., Mucs, D., Vinnars, M.-T., Papadogiannakis, N., Lindh, C.H., Andersen, C.Y., Damdimopoulou, P., 2019. Concentrations of perfluoroalkyl substances (PFASs) in human embryonic and fetal organs from first, second, and third trimester pregnancies. Environ. Int. 124, 482–492. https://doi.org/10.1016/J.ENVINT.2019.01.010.
Martin, M.T., Brennan, R.J., Hu, W., Ayanoglu, E., Lau, C., Ren, H., Wood, C.R., Corton, J.C., Kavlock, R.J., Dix, D.J., 2007. Toxicogenomic study of triazole fungicides and perfluoroalkyl acids in rat livers predicts toxicity and categorizes chemicals based on mechanisms of toxicity. Toxicol. Sci. 97, 595–613. https://doi.org/10.1093/toxsci/kfm065.
McLanahan, E.D., Andersen, M.E., Campbell, J.L., Fisher, J.W., 2009. Competitive inhibition of thyroidal uptake of dietary iodide by perchlorate does not describe perturbations in rat serum total T4 and TSH. Environ. Health Perspect. 117, 731–738. https://doi.org/10.1289/ehp.0800111.
Nelson, J.W., Hatch, E.E., Webster, T.F., 2010. Exposure to polyfluoroalkyl chemicals and cholesterol, body weight, and insulin resistance in the general U.S. population. Environ. Health Perspect. https://doi.org/10.1289/ehp.0901165.
NRC, 2007. Toxicity Testing in the 21st Century: A Vision and a Strategy. National Academies Press, Washington, DC https://doi.org/10.17226/11970.
NRC, 2009. Science and Decisions. National Academies Press, Washington, D.C. https://doi.org/10.17226/12209.
Palmer, C.N., Hsu, M.H., Griffin, K.J., Raucy, J.L., Johnson, E.F., 1998. Peroxisome proliferator activated receptor-alpha expression in human liver. Mol. Pharmacol. 53, 14–22. https://doi.org/10.1124/mol.53.1.14.
Paul, A.G., Jones, K.C., Sweetman, A.J., 2009. A first global production, emission, and environmental inventory for Perfluorooctane Sulfonate. Environ. Sci. Technol. 43, 386–392. https://doi.org/10.1021/es802216n.
Pérez, F., Nadal, M., Navarro-Ortega, A., Fàbrega, F., Domingo, J.L., Barceló, D., Farré, M., 2013. Accumulation of perfluoroalkyl substances in human tissues. Environ. Int. 59, 354–362. https://doi.org/10.1016/J.ENVINT.2013.06.004.
Renner, R., 2008. PFOS phaseout pays off. 4618 4618. Environ. Sci. Technol. 42. https://doi.org/10.1021/es0871614.
Rotroff, D.M., Wetmore, B.A., Dix, D.J., Ferguson, S.S., Clewell, H.J., Houck, K.A., LeCluyse, E.L., Andersen, M.E., Judson, R.S., Smith, C.M., Sochaski, M.A., Kavlock, R.J., Boellmann, F., Martin, M.T., Reif, D.M., Wambaugh, J.F., Thomas, R.S., 2010. Incorporating human dosimetry and exposure into high-throughput in vitro toxicity screening. Toxicol. Sci. 117, 348–358. https://doi.org/10.1093/toxsci/kfq220.
Seacat, A.M., Thomford, P.J., Hansen, K.J., Clemen, L.A., Eldridge, S.R., Elcombe, C.R., Butenhoff, J.L., 2003. Sub-chronic dietary toxicity of potassium perfluorooctanesulfonate in rats. Toxicology. https://doi.org/10.1016/S0300-483X(02)00511-5.
Seacat, A.M., Thomford, P.J., Hansen, K.J., Olsen, G.W., Case, M.T., Butenhoff, J.L., 2002. Subchronic toxicity studies on perfluorooctanesulfonate potassium salt in cynomolgus monkeys. Toxicol. Sci. 68, 249–264. https://doi.org/10.1093/toxsci/68.1.249.
Shao, K., Shapiro, A.J., 2018. A web-based system for Bayesian benchmark dose estimation. Environ. Health Perspect. 126, 017002. https://doi.org/10.1289/EHP1289.
Steenland, K., Tinker, S., Frisbee, S., Ducatman, A., Vaccarino, V., 2009. Association of perfluorooctanoic acid and perfluorooctane sulfonate with serum lipids among adults living near a chemical plant. Am. J. Epidemiol. 170, 1268–1278. https://doi.org/10.1093/aje/kwp279.
Sunderland, E.M., Hu, X.C., Dassuncao, C., Tokranov, A.K., Wagner, C.C., Allen, J.G., 2019. A review of the pathways of human exposure to poly- and perfluoroalkyl substances (PFASs) and present understanding of health effects. J. Expo. Sci. Environ. Epidemiol. 29, 131–147. https://doi.org/10.1038/s41370-018-0094-1.
Takacs, M.L., Abbott, B.D., 2007. Activation of mouse and human peroxisome proliferator-activated receptors (α, β/δ, γ) by perfluorooctanoic acid and perfluorooctane sulfonate. Toxicol. Sci. 95, 108–117. https://doi.org/10.1093/toxsci/kfl135.
Tan, Y.-M., Liao, K.H., Clewell, H.J., 2007. Reverse dosimetry: interpreting trihalomethanes biomonitoring data using physiologically based pharmacokinetic modeling. J. Expo. Sci. Environ. Epidemiol. 17, 591–603. https://doi.org/10.1038/sj.jes.7500540.
Thibodeaux, J.R., Hanson, R.G., Rogers, J.M., Grey, B.E., Barbee, B.D., Richards, J.H., Butenhoff, J.L., Stevenson, L.A., Lau, C., 2003. Exposure to Perfluorooctane Sulfonate during pregnancy in rat and mouse. I: Maternal and prenatal evaluations. Toxicol. Sci. 74, 369–381. https://doi.org/10.1093/toxsci/kfg121.
Thomas, R.S., Wesselkamper, S.C., Wang, N.C.Y., Zhao, Q.J., Petersen, D.D., Lambert, J.C., Cote, I., Yang, L., Healy, E., Black, M.B., Clewell, H.J., Allen, B.C., Andersen, M.E., 2013. Temporal concordance between apical and transcriptional points of departure for chemical risk assessment. Toxicol. Sci. 134, 180–194. https://doi.org/10.1093/toxsci/kft094.
Tice, R.R., Austin, C.P., Kavlock, R.J., Bucher, J.R., 2013. Improving the human hazard characterization of chemicals: a Tox21 update. Environ. Health Perspect. 121, 756–765. https://doi.org/10.1289/ehp.1205784.
U.S. EPA, 2016. Health effects support document for Perfluorooctane Sulfonate (PFOS). EPA 822-R-16-002. Washington, D.C., U.S. Environmental Protection Agency. Available: < https://www.epa.gov/sites/production/files/2016-05/documents/pfos_hesd_final_508.pdf > (accessed 1 August 2019).
Epa, U.S., 2009a. Long-Chain Perfluorinated Chemicals Action Plan. Environmental Protection Agency, Washington, D.C., U.S Available: https://www.epa.gov/sites/production/files/2016-01/documents/pfcs_action_plan1230_09.pdf.
Epa, U.S., 2009b. Provisional Health Advisories for Perfluorooctanoic Acid (PFOA) and Perfluorooctane Sulfonate (PFOS). Environmental Protection Agency, Washington, D.C. Available: https://www.epa.gov/sites/production/files/2015-09/documents/pfoa-pfos-provisional.pdf.
U.S. EPA, 2012. Benchmark Dose Technical Guidance. EPA/100/R-12/001. Risk Assessment Forum, U.S. Environmental Protection Agency, Washington, D.C.. Available: https://www.epa.gov/sites/production/files/2015-01/documents/benchmark_dose_guidance.pdf (accessed 1 August 2019).
UK COT, 2006. Committee on toxicity of chemicals in food, Consumer Products and the Environment: Cot Statement on the Tolerable Daily Intake for Perfluorooctane Sulfonate. Committee on Toxicity, London. Available: https://cot.food.gov.uk/sites/default/files/cot/cotstatementpfos200609.pdf.
UBA, 2016. HBM I values for Perfluorooctanoic acid (PFOA) und Perfluorooctanesulfonic acid (PFOS) in blood plasma: Statement of the German Human Biomonitoring Commission (HBM Commission). Bundesgesundheitsblatt. Gesundheitsforschung. Gesundheitsschutz. https://doi.org/10.1007/s00103-016-2437-1.
Wambaugh, J.F., Hughes, M.F., Ring, C.L., MacMillan, D.K., Ford, J., Fennell, T.R., Black, S.R., Snyder, R.W., Sipes, N.S., Wetmore, B.A., Westerhout, J., Setzer, R.W., Pearce, R.G., Simmons, J.E., Thomas, R.S., 2018. Evaluating in vitro-in vivo extrapolation of toxicokinetics. Toxicol. Sci. 163, 152–169. https://doi.org/10.1093/toxsci/kfy020.
Wan, H.T., Zhao, Y.G., Wei, X., Hui, K.Y., Giesy, J.P., Wong, C.K.C., 2012. PFOS-induced hepatic steatosis, the mechanistic actions on β-oxidation and lipid transport. Biochim. Biophys. Acta - Gen. Subj. 1820, 1092–1101. https://doi.org/10.1016/j.bbagen.2012.03.010.
Wang, L., Wang, Y., Liang, Y., Li, J., Liu, Y., Zhang, J., Zhang, A., Fu, J., Jiang, G., 2015. PFOS induced lipid metabolism disturbances in BALB/c mice through inhibition of low density lipoproteins excretion. Sci. Rep. 4, 4582. https://doi.org/10.1038/srep04582.
Watt, E.D., Judson, R.S., 2018. Uncertainty quantification in ToxCast high throughput screening. PLoS ONE 13, e0196963. https://doi.org/10.1371/journal.pone.0196963.
Wetmore, B.A., Wambaugh, J.F., Allen, B., Ferguson, S.S., Sochaski, M.A., Setzer, R.W., Houck, K.A., Strope, C.L., Cantwell, K., Judson, R.S., LeCluyse, E., Clewell, H.J., Thomas, R.S., Andersen, M.E., 2015. Incorporating high-throughput exposure predictions with dosimetry-adjusted in vitro bioactivity to inform chemical toxicity testing. Toxicol. Sci. 148, 121–136. https://doi.org/10.1093/toxsci/kfv171.
Wetmore, B.A., Wambaugh, J.F., Ferguson, S.S., Li, L., Clewell, H.J., Judson, R.S., Freeman, K., Bao, W., Sochaski, M.A., Chu, T.-M.M., Black, M.B., Healy, E., Allen, B., Andersen, M.E., Wolfinger, R.D., Thomas, R.S., 2013. Relative impact of incorporating pharmacokinetics on predicting in vivo zazard and mode of action from high-throughput in vitro toxicity assays. Toxicol. Sci. 132, 327–346. https://doi.org/10.1093/toxsci/kft012.
Wetmore, B.A., Wambaugh, J.F., Ferguson, S.S., Sochaski, M.A., Rotroff, D.M., Freeman, K., Clewell, H.J., Dix, D.J., Andersen, M.E., Houck, K.A., Allen, B., Judson, R.S., Singh, R., Kavlock, R.J., Richard, A.M., Thomas, R.S., 2012. Integration of dosimetry, exposure, and high-throughput screening data in chemical toxicity assessment. Toxicol. Sci. 125, 157–174. https://doi.org/10.1093/toxsci/kfr254.
World Health Organization (WHO); International Programme on Chemical Safety (IPCS), 2017. Guidance document on evaluating and expressing uncertainty in hazard characterization. World Health Organization, Geneva. Available: http://www.inchem.org/documents/harmproj/harmproj/harmproj11.pdf (accessed 1 August 2019).
Zeng, Z., Song, B., Xiao, R., Zeng, G., Gong, J., Chen, M., et al., 2019. Assessing the human health risks of perfluorooctane sulfonate by in vivo and in vitro studies. Environ. Int. 126, 598–610. https://doi.org/10.1016/J.ENVINT.2019.03.002.